To the Graduate Council:

I am submitting herewith a thesis written by Michael David Sanders entitled "Controlled Load Tests on a Four Girder Steel Bridge". I have examined the final copy of this thesis for form and content and recommend that it be accepted in partial fulfillment of the requirements for the degree of Master of Science, with a major in Civil Engineering.

J Harold Deatherage

Dr. James Harold Deatherage,
Major Professor

We have read this thesis
and recommend its acceptance:

Edwin G. Burdette

D.W. Goodpasture

Accepted for the Council:

CW Minkel

Associate Vice Chancellor
and Dean of The Graduate School

STATEMENT OF PERMISSION TO USE

In presenting this thesis in partial fulfillment of the requirements for a Master's degree at The University of Tennessee, Knoxville, I agree that the Library shall make it available to borrowers under rules of the Library. Brief quotations from this thesis are allowable without special permission, provided that accurate acknowledgment of the source is made.

Permission for extensive quotation from or reproduction of this thesis may be granted by my major professor, or in his absence, by the Head of Interlibrary Services when, in the opinion of either, the proposed use of the material is for scholarly purposes. Any copying or use of the material in this thesis for financial gain shall not be allowed without my written permission.

Signature Michael [signature]

Date 12/28/93

Controlled Load Tests on a Four Girder Steel Bridge

A Thesis
Presented for the
Master of Science
Degree
The University of Tennessee, Knoxville

Michael David Sanders

May 1994

ACKNOWLEDGEMENTS

I would like to thank my major professor, Dr. Hal Deatherage, for his patience and guidance. I would also like to think the other members of my committee, Dr. Ed Burdette and Dr. David Goodpasture. The assistance of these three people has been invaluable over the past years. Their commitment to the engineering field and to the education of their students is sincerely appreciated. I would also like to thank my wife, Sandi. Her patience and understanding during some very stressful times provided me with the encouragement needed to complete this thesis.

ABSTRACT

The Holston River Bridge project provided an excellent opportunity to examine the response of an actual structure to applied loads. During the course of the project response to both actual traffic loading and to controlled loading was measured. This thesis examines the data collected during the controlled load tests and outlines the means by which it was collected.

Methods currently used to distribute applied loads to the main structural members have been found to produce very conservative results in several cases. This project made it possible to compare actual measured response to the response calculated by various means. The measured responses were compared to AASHTO values and to values calculated by a method developed by another researcher. The later, an extension of the Guyon-Massonet method, was found to produce less conservative but more accurate results than the AASHTO method.

Full speed and crawl test data were analyzed in order to calculate dynamic impact factors for this structure. These values were also compared to the values used by AASHTO.

TABLE OF CONTENTS

LIST OF TABLES

LIST OF FIGURES

LIST OF SYMBOLS

Notation	Description
2b	width of equivalent bridge
b_1	spacing of longitudinal girders
B_G	flexural stiffness of each longitudinal girder
B_D	flexural stiffness of each transverse diaphragm
C_G	torsional stiffness of each longitudinal girder
C_D	torsional stiffness of each transverse diaphragm
E_G	modulus of elasticity of girder
E_D	modulus of elasticity of deck
f_c	compressive strength of concrete
f_y	yield strength of steel
J_G	polar moment of inertia of girder
J_D	polar moment of inertia of decks
K	distribution coefficient

Notation	Description
L	span of bridge
P	intensity of load
t	thickness
α	torsion parameter
θ	flexural stiffness parameter
ρ_G	flexural stiffness per unit width of equivalent bridge
ρ_D	flexural stiffness per unit length of equivalent bridge
Y_G	torsional stiffness per unit width of equivalent bridge
Y_D	torsional stiffness per unit length of equivalent bridge

CHAPTER I

INTRODUCTION

1.1 Description

The Holston River Bridge carries Interstate Forty over the Holston River just east of Knoxville, Tennessee. The bridge supports six lanes of traffic, three in each direction. Four continuous steel girders support a seven and one half inch concrete deck which acts compositely with the girders. The roadway shoulder is supported by cantilever plates which frame into the web of the exterior girders (Figure 1.1). The girders vary in depth throughout the length of the bridge, but are identical at any given cross section. 1193 feet in total length, the bridge consists of seven spans ranging in length from 135 feet to 240 feet (Figure 1.2). Within the single 240 foot span the girders are connected laterally by cross trusses at 22 feet on center (Figure 1.3). In all other spans floor beams span between the girders (Figure 1.4). Both the trusses and floor beams support two wide flange

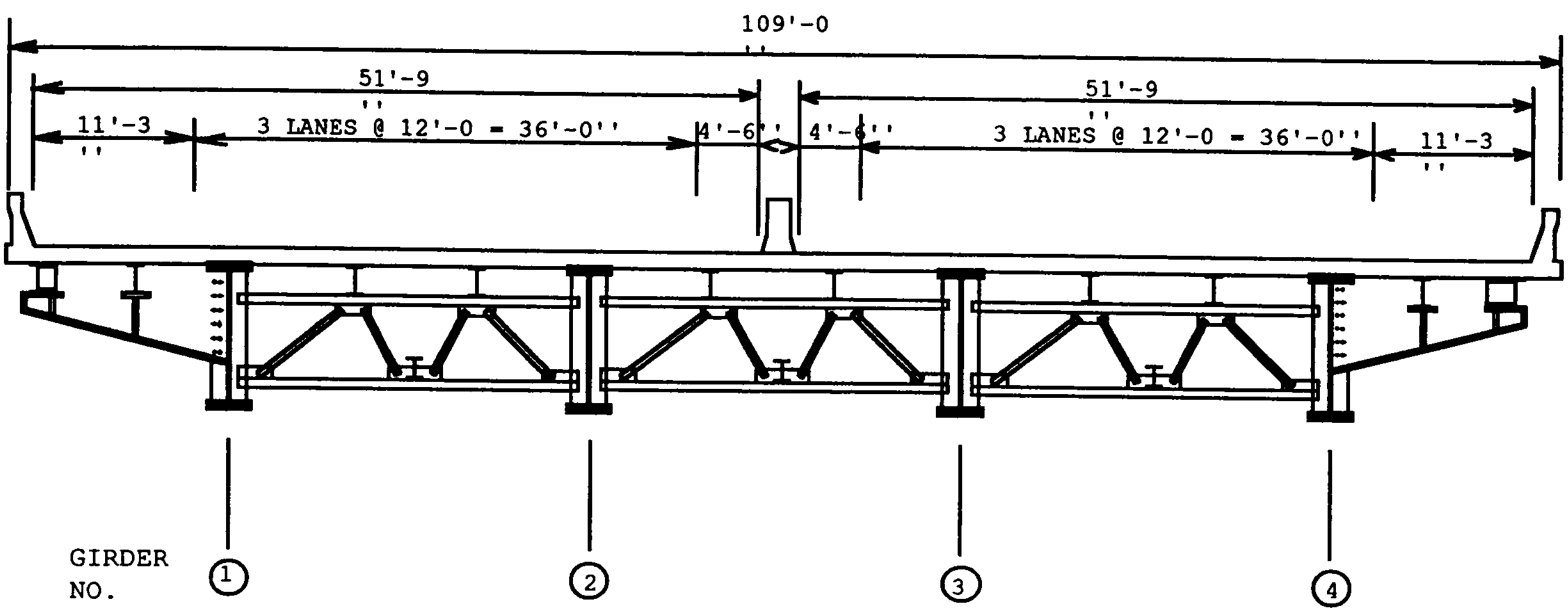

Figure 1.1 - Typical Cross Section

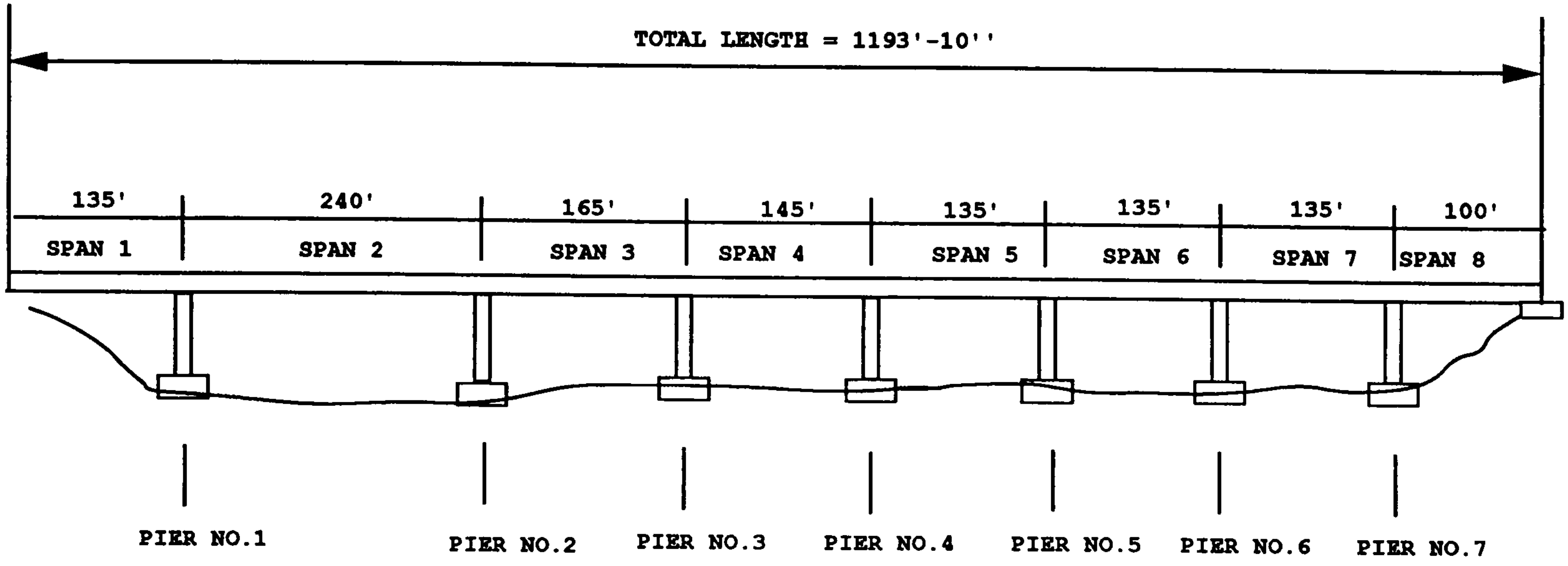

Figure 1.2 - Elevation View

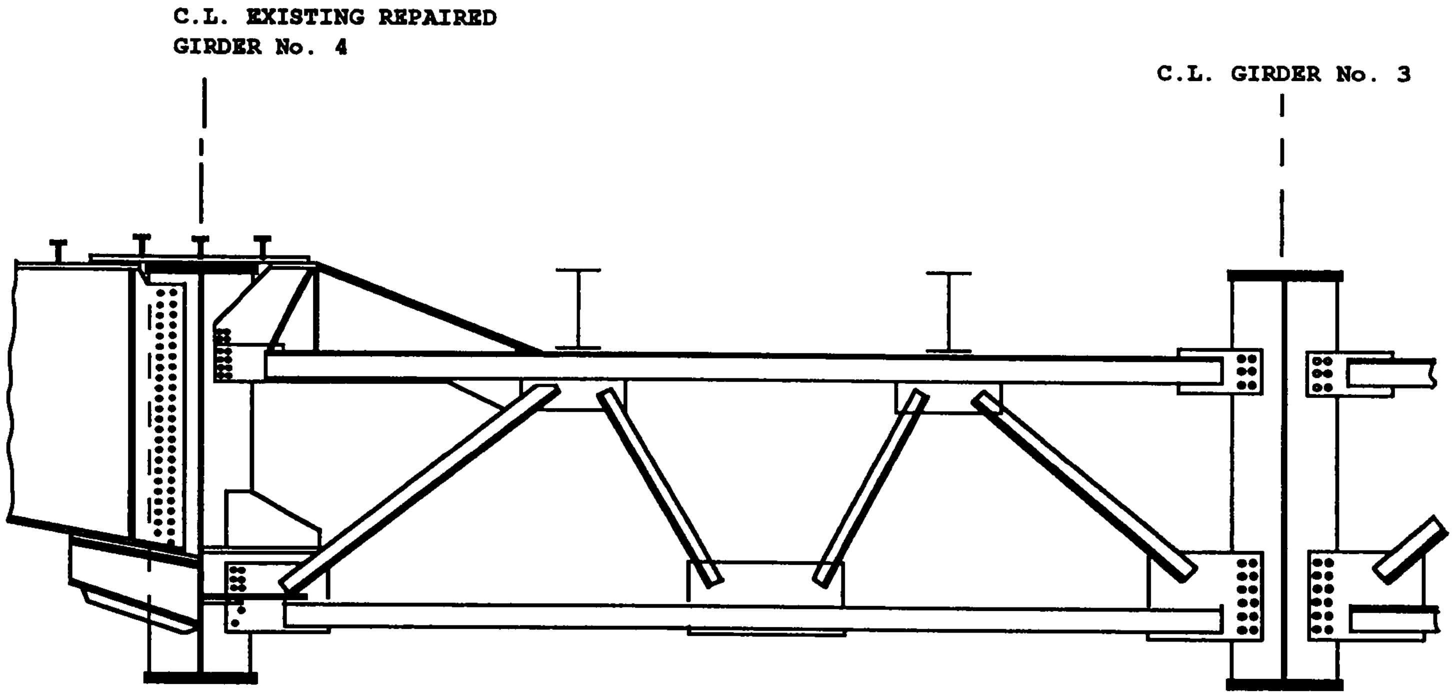

Figure 1.3 - Typical Floor Truss

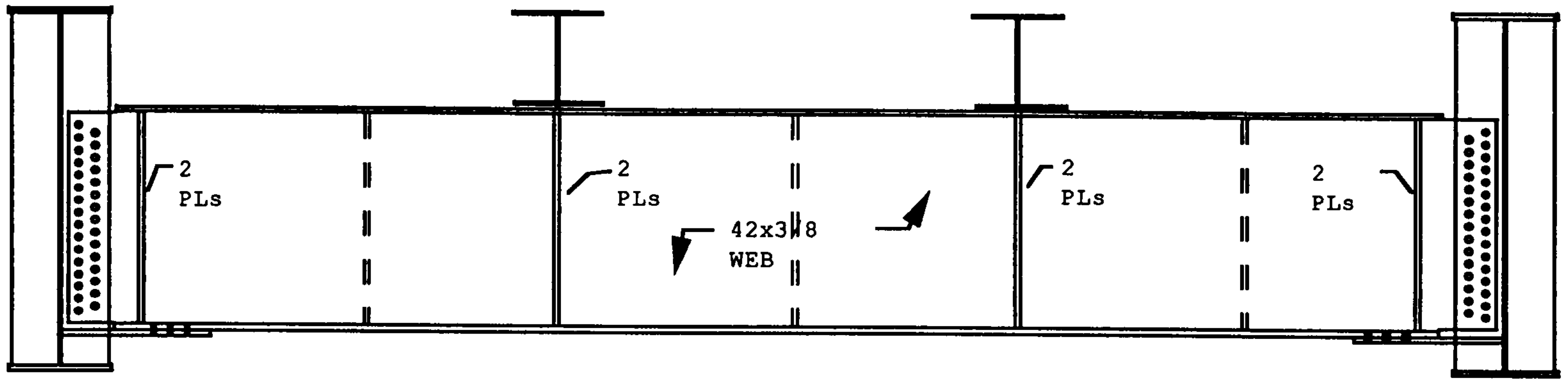

STIFFNERS ARE 3X5/16'' PLATES

Figure 1.4 - Typical Transverse Floor Girder

sections each. These wide flange sections serve as stringers for the bridge deck.

1.2 Background

In January 1992, the Tennessee Department of Transportation discovered a fatigue failure in the outside girder on the east bound lane (girder number 4). The fracture was located near the one-third point of the 240 foot span between piers one and two directly over the main channel of the river (Figure 1.5). The fracture extended almost the entire depth of the member. A large gap was present at the bottom flange of girder number four. The outside two lanes of the bridge were immediately closed to traffic on each side. Measures were then taken to repair the damaged girder. A retrofit of the cantilever to girder web connection was also implemented. This was intended to eliminate the out of plane distortion of the girder web which initiated the failure. In January 1993, a research project was begun by the University of Tennessee Transportation Center to investigate the Holston River Bridge fatigue failure. This Project had four objectives which were spelled out by a proposal to the Tennessee Department of Transportation. These objectives were (1) determine the

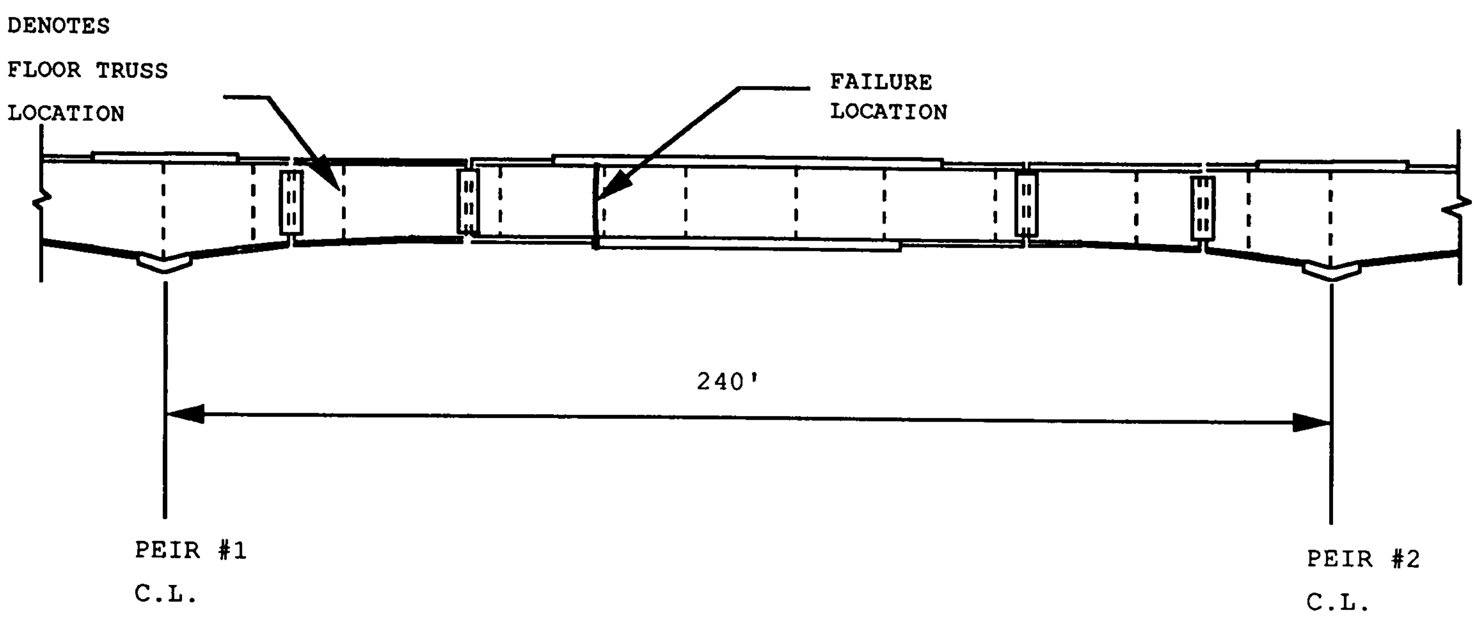

Figure 1.5 - Elevation of Girder Number 4 in Span 2

effects of the retrofit repairs, (2) estimate the portion of the bridge fatigue life expended at the time of failure, (3) estimate the remaining life of the bridge based on current and estimated future usage and identify controlling fatigue detail locations, (4) study critical details of the bridge structure for potential fatigue problems resulting from dynamic response of the structure. In order to accomplish these objectives extensive field testing was required. First, careful inspection of the bridge plans and the bridge itself revealed the location of several critical points of interest. Members at these locations were then instrumented with strain gages. Strain gage data were collected under both normal traffic and controlled loads. The information from these gages was used to determine the response of the structure under these loads. Stress ranges at fatigue prone details were examined in great detail. Particular attention was given to the lateral gusset plate located at the bottom floor truss to girder connection.

1.3 Objective

This thesis provides a summary of the controlled load tests performed on the Holston River Bridge. The reasons for the project as well as the methods used during the project are outlined in this thesis. The structural behavior of the bridge when subjected to a controlled load was examined in detail. Lateral distribution of these loads to the four longitudinal girders was examined. The measured distributions were compared with distributions obtained by analytical methods(24) and those recommended by AASHTO. The results of both the dynamic and static controlled load tests were analyzed. These data were then compared in order to determine a dynamic impact factor for the structure. These values were also compared to AASHTO values.

CHAPTER II

REVIEW OF LITERATURE

2.1 Fatigue Prone Details

Over the past three decades fatigue cracking has been associated with a number of localized failures of bridge components. These fatigue cracks have initiated at various details common on welded structures. These fatigue prone details have been the subject of much research in the past(6,7,8,9,10,11,12,13,14,19,20). Many factors have been found to contribute to the severity of fatigue cracking. A review of literature which examines these various factors follows in this section.

A study of the Lafayette Street Bridge in St. Paul Minnesota was begun when a crack was discovered in one of the main girders(13). This structure illustrated the problem of intersecting welds at connections of transverse members. The cause as well as appropriate retrofit procedures were examined in detail.

Lee, Yen, Fisher, and Castiglioni analyzed a four span continuous five steel girder interstate bridge in

Pennsylvania in order to determine fatigue damage at certain details(20). Forces in diaphragm members were examined with respect to the location of loads. The forces and displacements at selected connection plates were also examined. These results were compared to field measurements. Retrofitting procedures for the web gaps subject to distortion induced fatigue cracking were presented.

Retrofitting techniques can be classified as those applicable to load-induced fatigue cracking, distortion induced fatigue cracking, or both(12). Fisher suggests in order to determine the appropriate retrofit, the phenomenon producing the cracking must be identified. Orientation of the cracks can assist in this identification. various retrofit procedures have been examined by Fisher(12).

Fatigue cracking on Interstate Seventy Nine bridges in West Virginia was investigated by Kulicki, Murphy, Mertz, and Fisher(19). The design of the Interstate Seventy Nine bridges are similar to that of the Holston River Bridge. Two continuous steel girder structures were found to have load and displacement induced fatigue cracking. The need to distinguish between cracking perpendicular and cracking parallel to stress fields is emphasized in their report. The need to determine the phenomenon responsible for the cracks is also illustrated.

Cases of distortion induced fatigue cracking have been examined by Fisher, Yen, and Wagner(11). The orientation of fatigue cracks with respect to the in plane flexural bending stresses was shown to be an important factor. This orientation is the deciding factor in the rate of crack growth.

In the National Cooperative Highway Research Program(NCHRP) Report 227(14) details susceptible to fatigue cracks at weld toes were evaluated. Particular attention was given to lateral connection plates. Recommendations were made for the revision of the AASHTO <u>Standard Specifications for Highway Bridges</u>. Retrofitting procedures were also discussed for the various details.

Keating and Fisher(18) reviewed several fatigue studies of AASHTO details in order to develop a computerized database. This database contained fatigue test results of various detail types. A review of the data indicated several detail types had not been properly accounted for by AASHTO. Revisions to the AASHTO

Standard Specifications for Highway Bridges were recommended.

Laboratory tests of eight full size welded plate girders were conducted by Fisher(7). These girders were fitted with various web attachments representing different categories of fatigue details. The results of these tests were used to establish a new recommended lower bound for some AASHTO fatigue curves.

Several details present on the Holston River Bridge have been studied by Fisher. The connections of transverse components in multigirder bridges including floor beam and floor truss connections have been examined in detail(10). Methods for preventing cracking at and retrofitting these details are also studied.

Fisher has examined end restraint, copes, and flange terminations as factors that promote fatigue cracking(6). The termination of flanges of built up members outside their end connection is common. This is shown to be a location prone to fatigue cracking. The various factors contributing to the formation of these cracks are discussed in detail by Fisher(6). The connections of the floor beams in the Holston River Bridge have details of this type.

2.2 Dynamic Impact Factors

Data including dynamic impacts and girder distributions were collected and incorporated into a system to evaluate bridge safety by Ghosn, Moses, and Gobieski(15). Dynamic impact factors calculated from these data were compared to AASHTO values. The AASHTO values were found to be conservative.

Dynamic impact factors are considered in NCHRP Report 301(22). Impact factors are given for various sites. These were taken from a database of previous studies. It was determined that impact was directly related to roadway roughness. Instructions are provided for selecting categories for a given roadway.

The effect of truck weight on the dynamic impact factor was examined by Nowak(25). It was found that as truck weight increased the dynamic impact factor decreased.

2.3 Lateral Load Distribution

Present AASHTO distribution factors have been found to be conservative by many researchers(5,17,21,23). This research has encompassed different means including analytical methods, computer models, scale models, and actual field measurements. The work by Sanders and

Elleby referenced Guyon and Massonet extensively in developing the current AASHTO load distribution factors. Deatherage(5) extended the Guyon-Massonnet theory to develop a series of influence coefficients which more accurately represent the effects of a load applied laterally on the cross section of a bridge. In Deatherage's work a torsional parameter, α, and a flexural stiffness parameter, θ, are used to determine the appropriate influence coefficients to be used with a particular structure.

The effect of different variables on lateral distribution were examined by Hays, Sessions, and Berry(17). This was accomplished through the use of a computer program, Structural Analysis for Load Distribution(SALOD). AASHTO factors were found to produce conservative results when compared to the results from SALOD.

An experimental test program was used to evaluate the behavior of a four tenths scale model of a two span continuos plate girder bridge(21). Distribution factors computed using AASHTO procedures were found to be quite conservative for the interior girder and less so for the exterior girders.

Field data have been collected using strain gages and weigh in motion(WIM) equipment(23). These data have been used to calculate lateral distribution factors and dynamic impact factors. When compared to AASHTO values, the AASHTO values are again found to produce conservative results.

Nowak, Nassif, and Frank(24) also used strain gages and WIM equipment to evaluate a structures response to traffic. The structure is a multi-span bridge supported by four steel plate girders. In addition to evaluation of the bridge details with respect to fatigue damage, measured girder moment distribution factors are presented for the structure.

CHAPTER III

EVALUATION OF THE HOLSTON RIVER BRIDGE

3.1 Introduction

After discovery of the fracture, procedures were initiated immediately to repair the damaged girder. When the repair was complete, efforts were made to identify and correct the cause of the failure. At this time it was believed the failure was caused by out of plane distortion induced by the cantilever bracket attached to the girder web. A retrofit of the bottom cantilever connection was instituted to eliminate this problem.

Evaluation of the bridge details at the beginning of this study led to the discovery of a more likely cause of the fracture. The connection of the bottom chords of the transverse floor truss to the girder web created a web gap between a vertical stiffener and a lateral gusset plate. This web gap is discussed in detail in section 3.3. Other fatigue prone details were also identified during examination of the bridge and are discussed in section 3.3.

3.2 Fracture Repair and Retrofit

Immediately after the discovery of the fracture and closing of the outside traffic lanes, actions were taken to repair the damaged girder. Several large high strength bolts were attached to the bottom flange of the girder. Four steel girders were placed on the bridge deck directly above the fracture location. These girders were connected to the bridge girder with hanger rods. Hydraulic rams were then used to jack the girder back into place. While lifted from above by the hanger rods the bolts on the bottom flange were tightened. The gap in the girder was closed as much as possible by this method. The girder was then welded back together. Splice plates were added to further strengthen the repair. Plates were bolted to both sides of the bottom flange and to both sides of the girder web (Figure 3.1). This method did reduce the deflection of the fractured girder; however, it did not completely eliminate it. The deflection of the bridge deck is still quite noticeable. During rainy weather this is more evident due to the ponding of water directly above the fracture location.

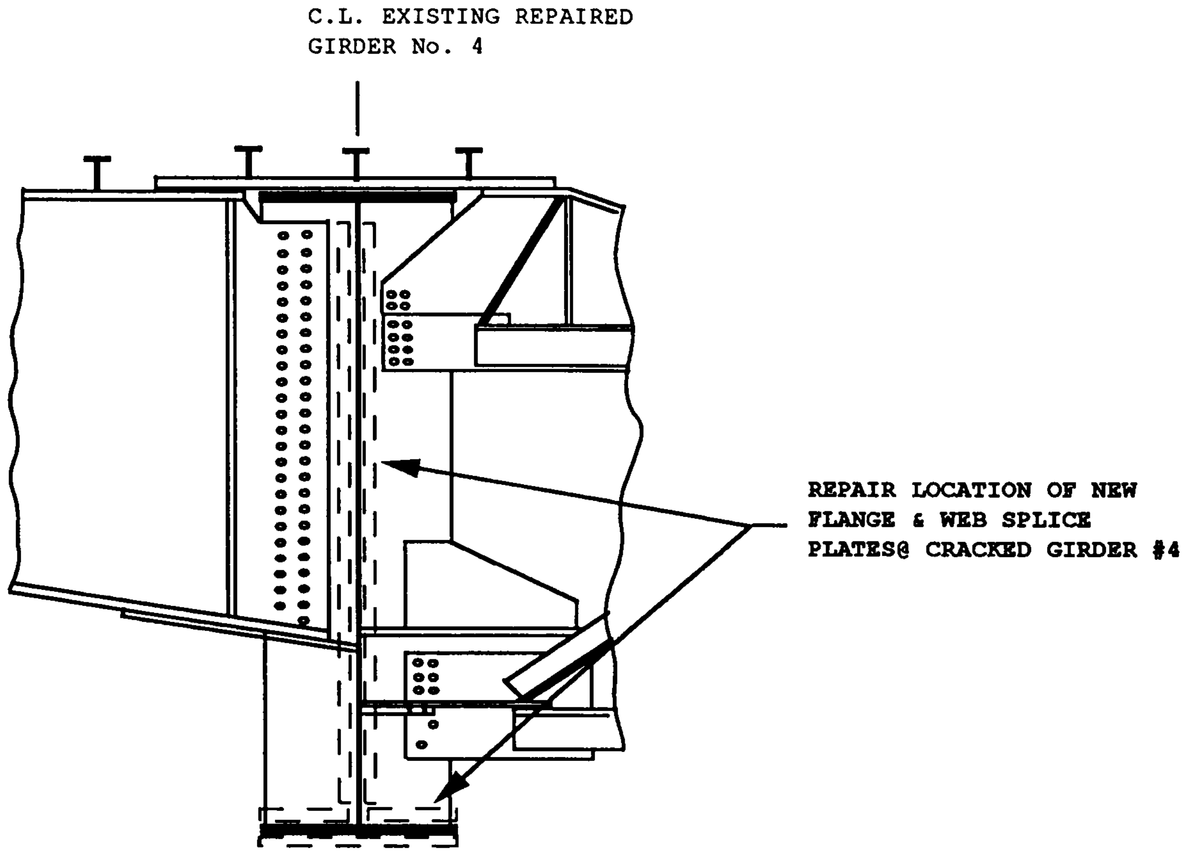

Figure 3.1 - Repair Plates at Failure Location

This ponding however is confined to the shoulder lane and is most likely not significant enough to cause any problems to the structure or to traffic.

After the repair of the girder fracture was complete, additional repair and retrofitting of the bridge began. Other cracks were present in the girder web besides the main fracture. Adjacent locations were also found to have damaged components. This damage included cracks in gusset plates of the floor truss at the fracture and damaged connections at adjacent floor trusses. Holes drilled to arrest the growth of cracks near the fracture location are visible (Figure 3.2). Bent gusset plates and loose bolts are also still evident at adjacent floor truss locations.

A retrofit of the cantilever to girder flange connection was used to eliminate the situation that was believed responsible for the fracture in girder number four. At the time of the failure it was believed to have been initiated by out of plane forces exerted on the girder web at the bottom of the cantilever to girder connection. Before retrofitting, the bottom flange of the cantilever bracket was connected to the girder web at a point approximately one and one half feet above the

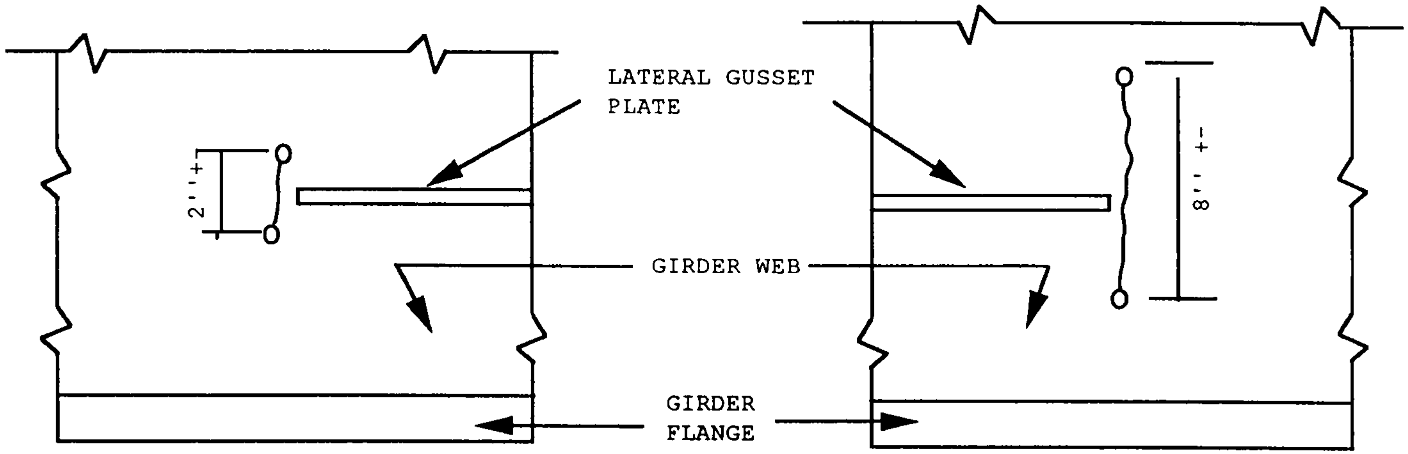

Figure 3.2 - Fatigue Cracks and Retrofit Holes at Ends of Lateral Gusset Plate on Interior of Girder Number 4

bottom floor truss to girder connection, located on the opposite side of the girder web (Figure 3.3). The retrofit consisted of attaching a new plate to the bottom flange of the cantilever bracket. The new plate extended the bottom of the cantilever to girder connection down one and one half feet. The bottom gusset of the retrofit plate now connects to the girder web directly opposite the bottom floor truss to girder connection (Figure 3.4). The intent of this measure was that any forces from the cantilever would now be transferred directly into the floor truss. With the girder web stiffened at the bottom cantilever connection by the floor truss, out of plane distortion is thereby greatly reduced. Another consequence of the retrofit is that the bottom lateral gusset plate of the new plate backs up the web gap created on the opposite side of the girder web at the floor truss connection. This web gap situation, not the cantilever connection, was later determined to be the most probable cause of the fatigue cracking that initiated the fracture in girder number four. The specifics of this web gap detail are discussed in depth in the next section of this chapter.

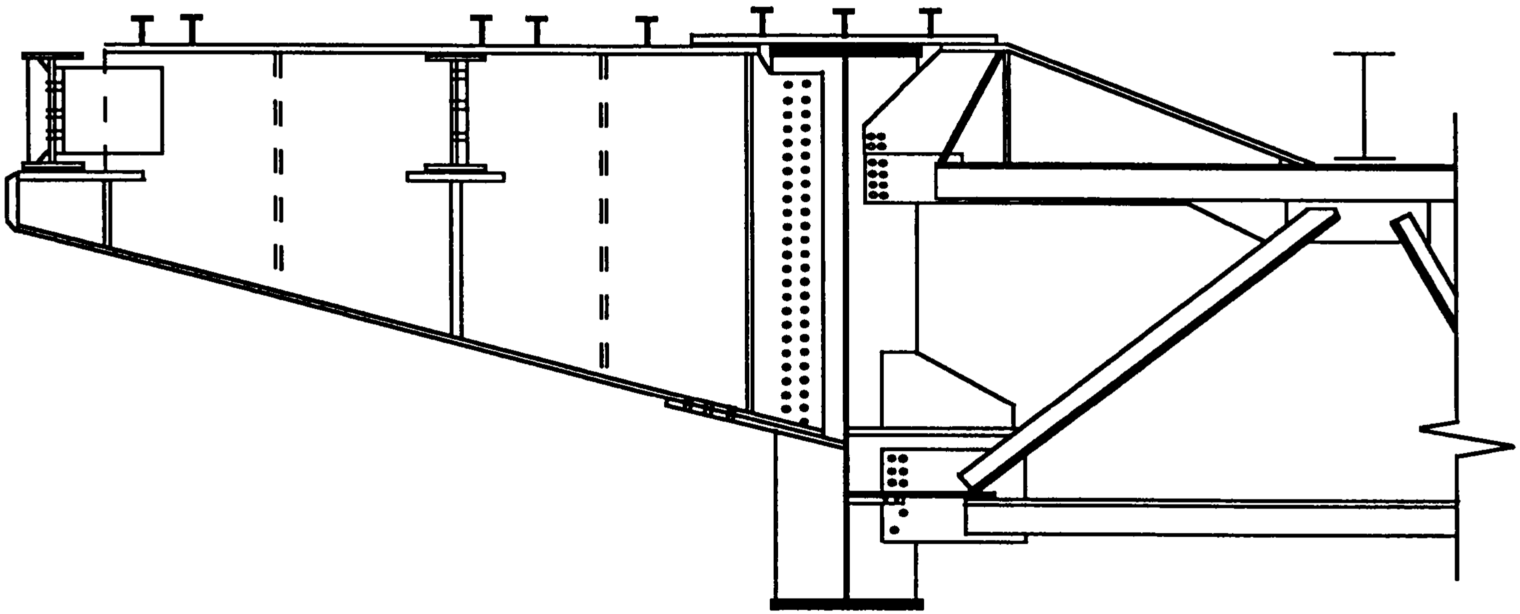

Figure 3.3 - Cantilever to girder Connection Prior to Retrofit

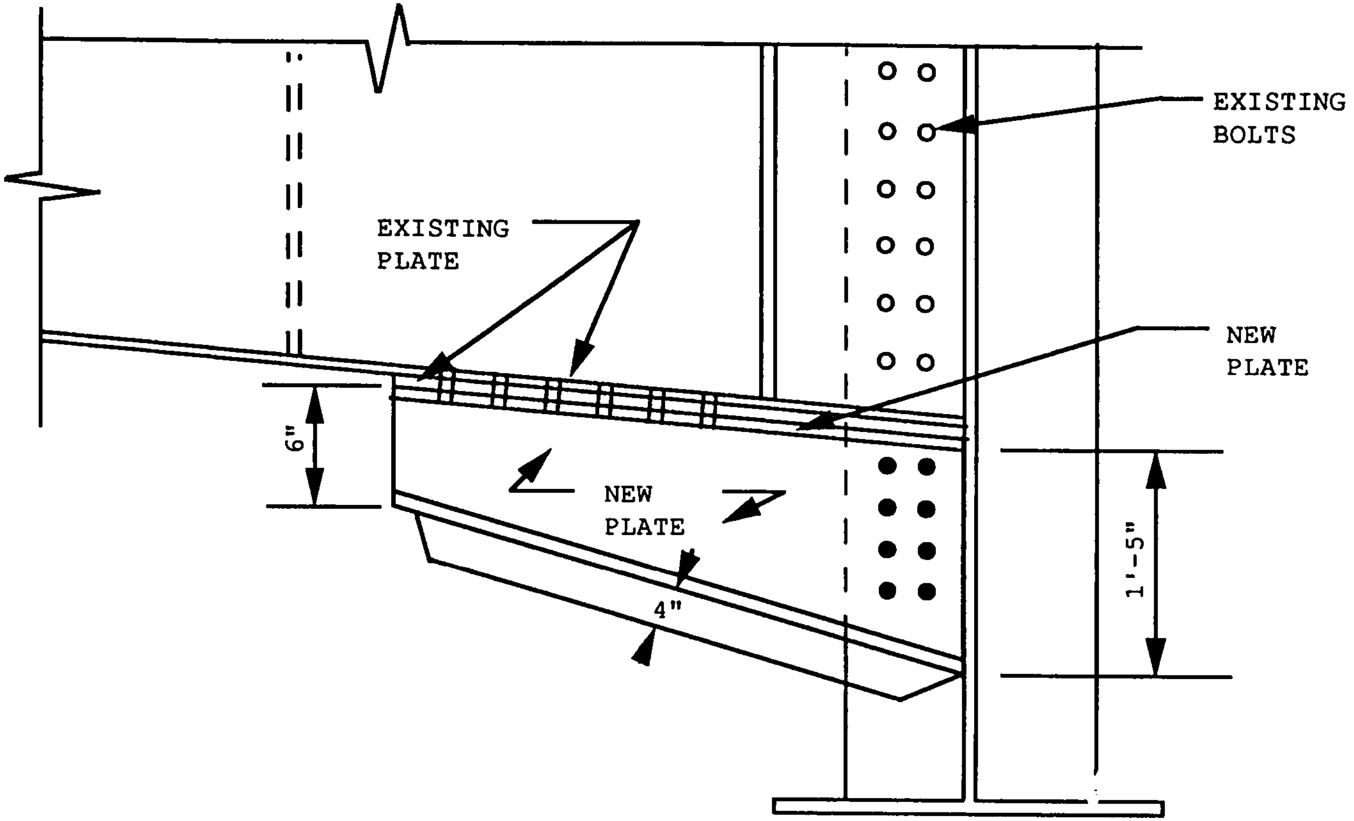

Figure 3.4 - Cantilever to Girder Connection with Retrofit Plate in Place

3.3 Identification of Fatigue Prone Details

The fatigue performance of any structure is governed by the amount of fatigue resistance present at details located within that structure. The fatigue category of these details along with the number and magnitude of loading cycles they are subjected to serve to determine the fatigue life of a structure. Therefore, one of the first steps in this study was the identification of fatigue prone details within the bridge. First, a review of literature was undertaken to determine the types of details found to have been a problem in other structures. An examination of the bridge plans and the structure itself was conducted to locate any low fatigue resistant details present in this structure. In addition to the research staff of this project Dr. John W. Fisher was consulted on the matter of identification of these problem details. Dr. Fisher is most likely the premier expert in steel bridge fatigue research in this country. His expertise was invaluable during an initial inspection of the structure. This inspection was for the purpose of determining the location of strain gages that would be used to determine the stress ranges at given locations.

Span two is the longest, and is unique, compared to the other spans of this bridge. Transverse floor truss frames span between the four girders within this span. These trusses support wide flange sections that serve as stringers for the bridge deck and transfer their loads into the main girders (Figure 3.5). All other spans use welded built up floor girders for this purpose (Figure 3.6). Several fatigue prone details were found to exist within these floor trusses and their connections to the girders.

The bottom connection of the floor truss to girder web connection is a major point of interest in this project. The lateral gusset plate that serves to connect the bottom chords of the truss and the bridge's diagonal X-bracing to the web of the girder is notched to accommodate the vertical stiffener located on the web (Figure 3.7). This detail solves the problem of intersecting welds at the gusset stiffener intersection. The gusset is bolted to tabs that are welded horizontally along the web of the girder on each side of the vertical stiffener. These tabs end four inches from the vertical stiffener. This forms a four inch web gap on each side of the vertical stiffener (Figure 3.8). This web gap is a length of unstiffened web that is subject to out of plane distortion. Forces introduced by the floor truss tend to pump the girder web in and out. When out of

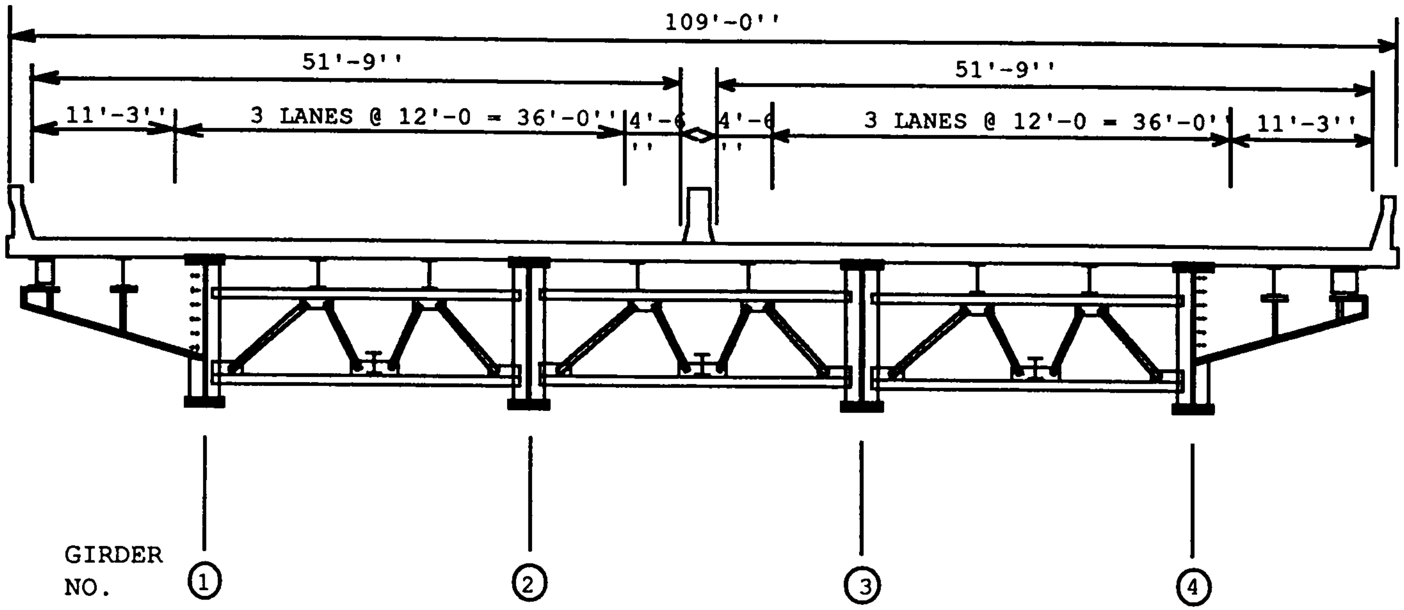

Figure 3.5 - Typical Cross Section in Span 2

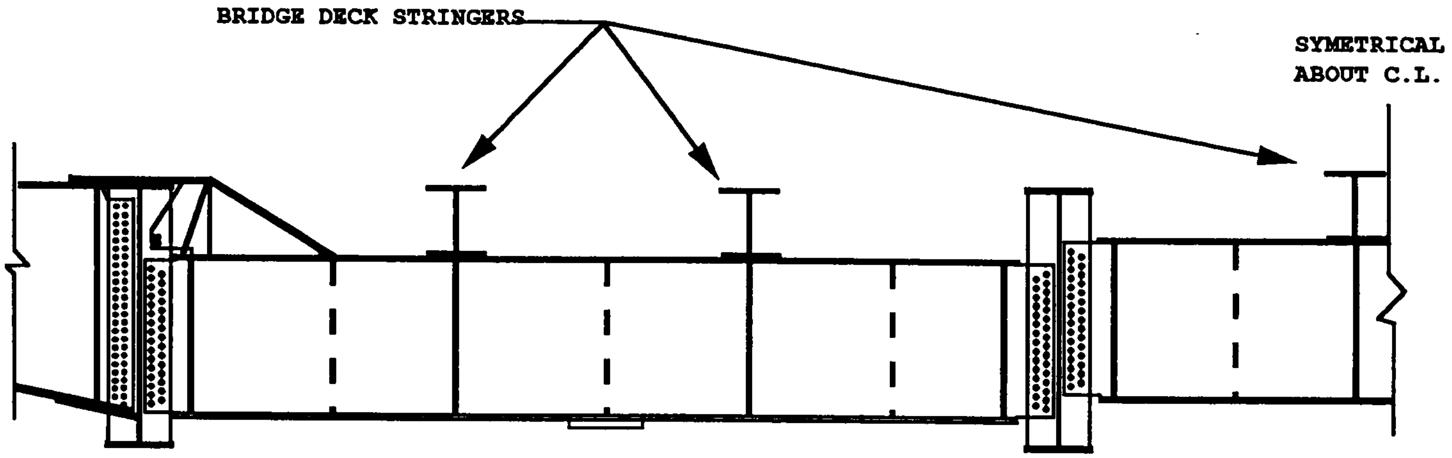

Figure 3.6 - Typical Cross Section at Floor Girder Location

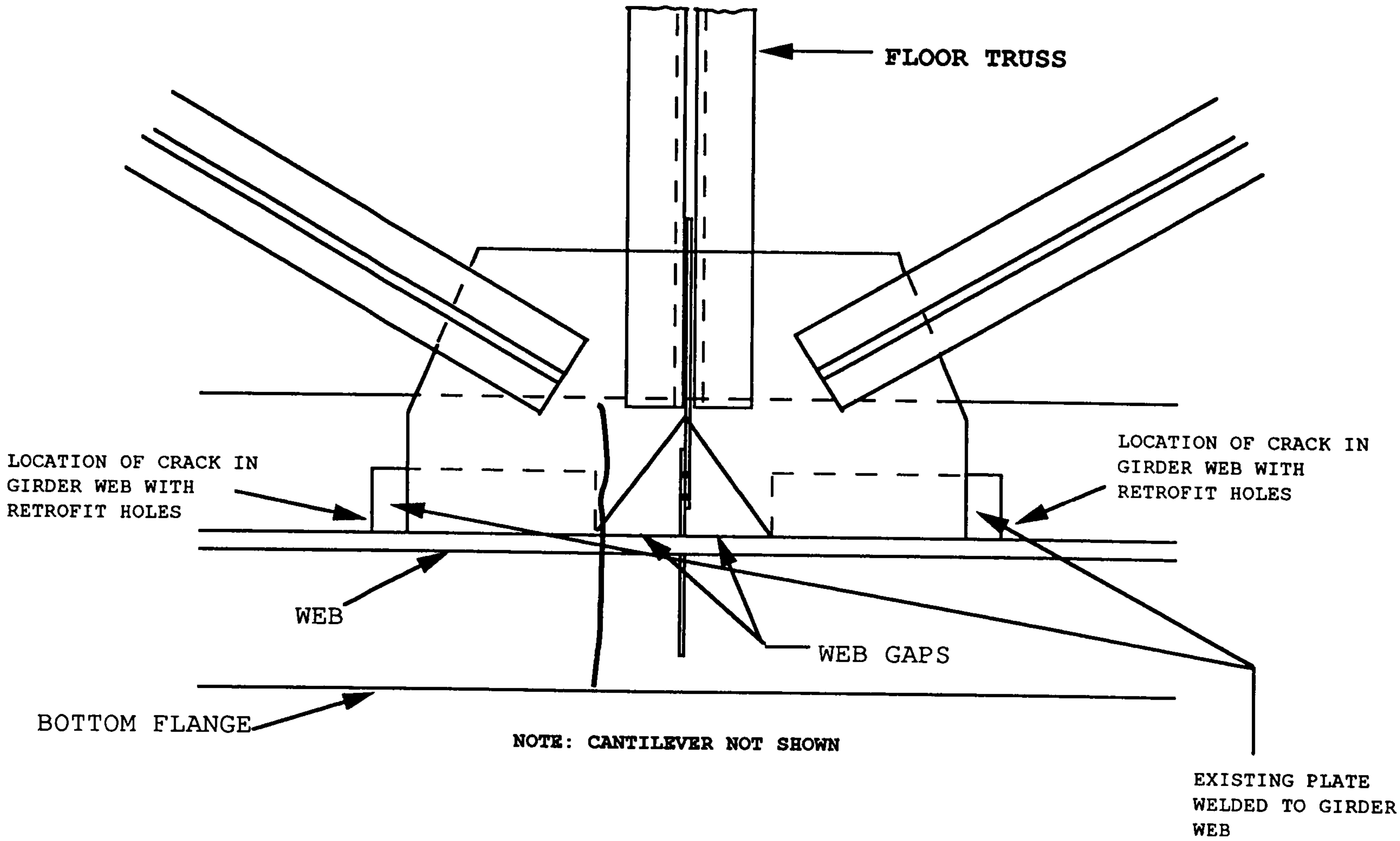

Figure 3.7 - Notch in Gusset Plate at Bottom Floor Truss to Girder Web Connection

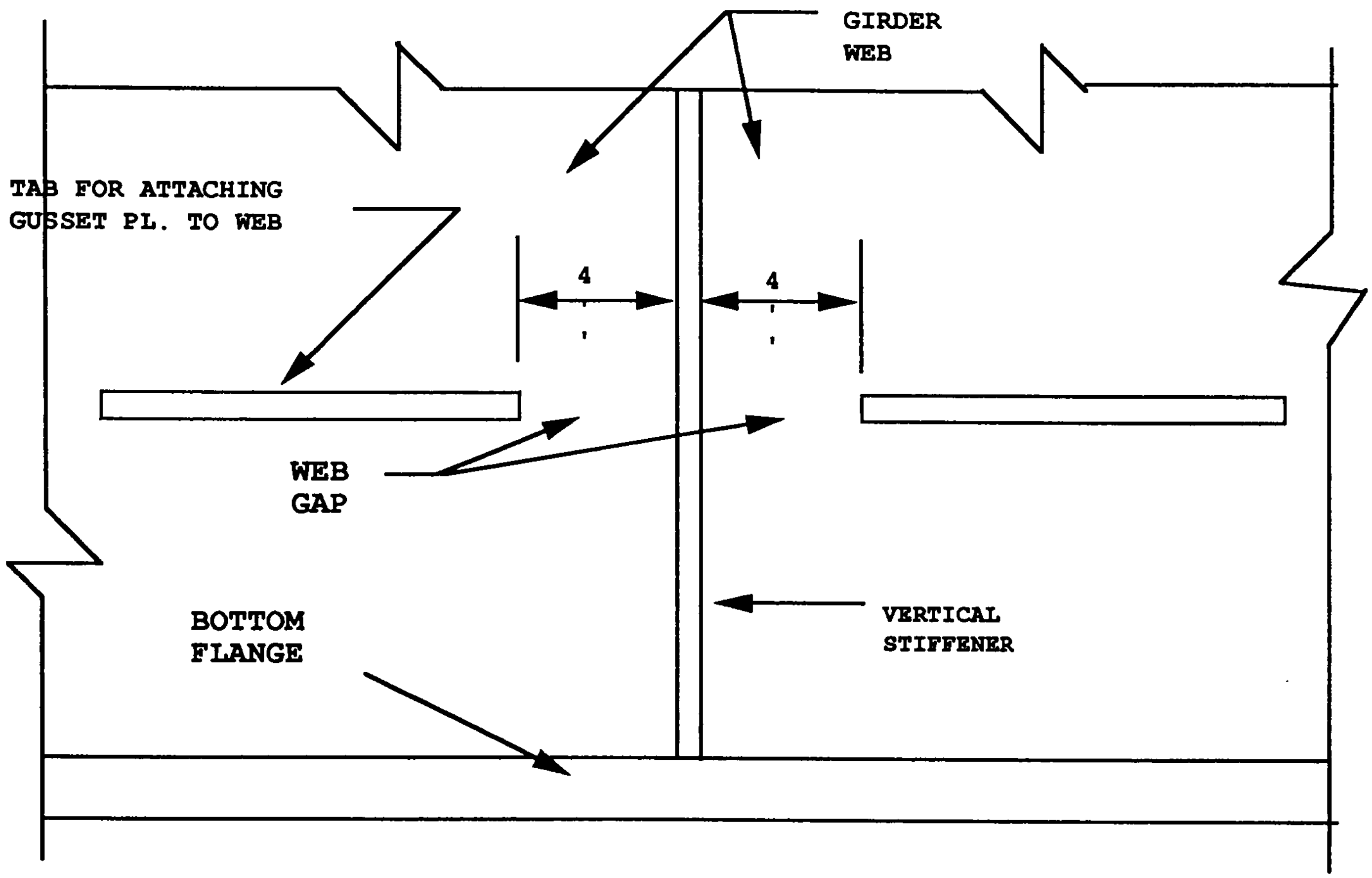

Figure 3.8 - Web Gap on Flange of Exterior Girder

plane distortion occurs, this portion of the web behaves similarly, to a beam with two fixed ends, put into double curvature, and having a length of four inches. This detail is classified as a category E, but considering the small gap involved, performance may be worse than that of category E (16). Small out of plane distortion over this short distance can result in high stress ranges within this gap.

This out of plane distortion within the web gap was determined to be the most likely cause of the girder failure. During the last thirty years hundreds of bridges have developed fatigue cracks to some degree. The largest category of this cracking is a result of unequal out-of-plane displacements across small sections of girder webs(6). Cracking usually extends along the weld toes and perpendicular to maximum stresses(11). In a case such as this, where a horizontal web gap is present, the problem is particularly serious. In-plane bending stresses are in the same direction as the secondary out-of-plane stresses that cause the cracks. Cracks due to the out-of-plane stresses then tend to form perpendicular to the flexural bending stresses (i.e. vertical). With the crack oriented in this manner it would continue propagating due to the cyclic flexural stresses, resulting in fracture of the girder. In this situation the growth of the crack could be relatively rapid(11).

This type of detail can be retrofitted in one of two manners. The web gap can be made more flexible to accommodate the displacement more uniformly and thus reduce the concentration of the displacement-induced stress, or can be made stiffer to eliminate the localized distortion(12). The retrofit of the cantilever to girder connection discussed earlier serves to accomplish the latter of these solutions. The bottom lateral gusset plate on the new cantilever connection serves to back up the web gap. Located directly opposite the web gap the new gusset plate bridges the web gap and thereby eliminates the out-of-plane distortion of the web gap. All locations on the bridge with this detail received the retrofit plate. This eliminated the situation that existed before the girder failure. With the study being unable to establish experimentally the stress ranges present prior to the retrofit, the focus of data collected at this location was somewhat hampered. However, the determination of the adequacy of the retrofit was still possible.

All floor truss members are made of double angles. Within the floor trusses several gusset plates are inserted between the chords of the truss. The chords are welded to the gussets. This was determined to be a Category E detail. Strain gages were located to record stress ranges in the various chords of the truss. This allows determination of the likelihood of a fatigue crack developing here.

A similar detail is also present at the floor girder locations (Figure 3.9). At the connection of the floor girder to the fascia girders the bottom cantilever gusset plate backs up the web gap. However, at the floor girder to interior girder connection the web gap is unstiffened on the other side of the web. This web gap was instrumented in order to determine if high out-of-plane stresses were present. In addition to the web gap, strain gages were also placed on the web to detect any out-of-plane distortion at the end of the lateral gusset plate.

Coped flanges of floor girders have been developing cracks in other structures. The floor girders on this bridge have their flanges terminating near the end connections to the girders. The termination of the girder flange to web weld at this point results in a

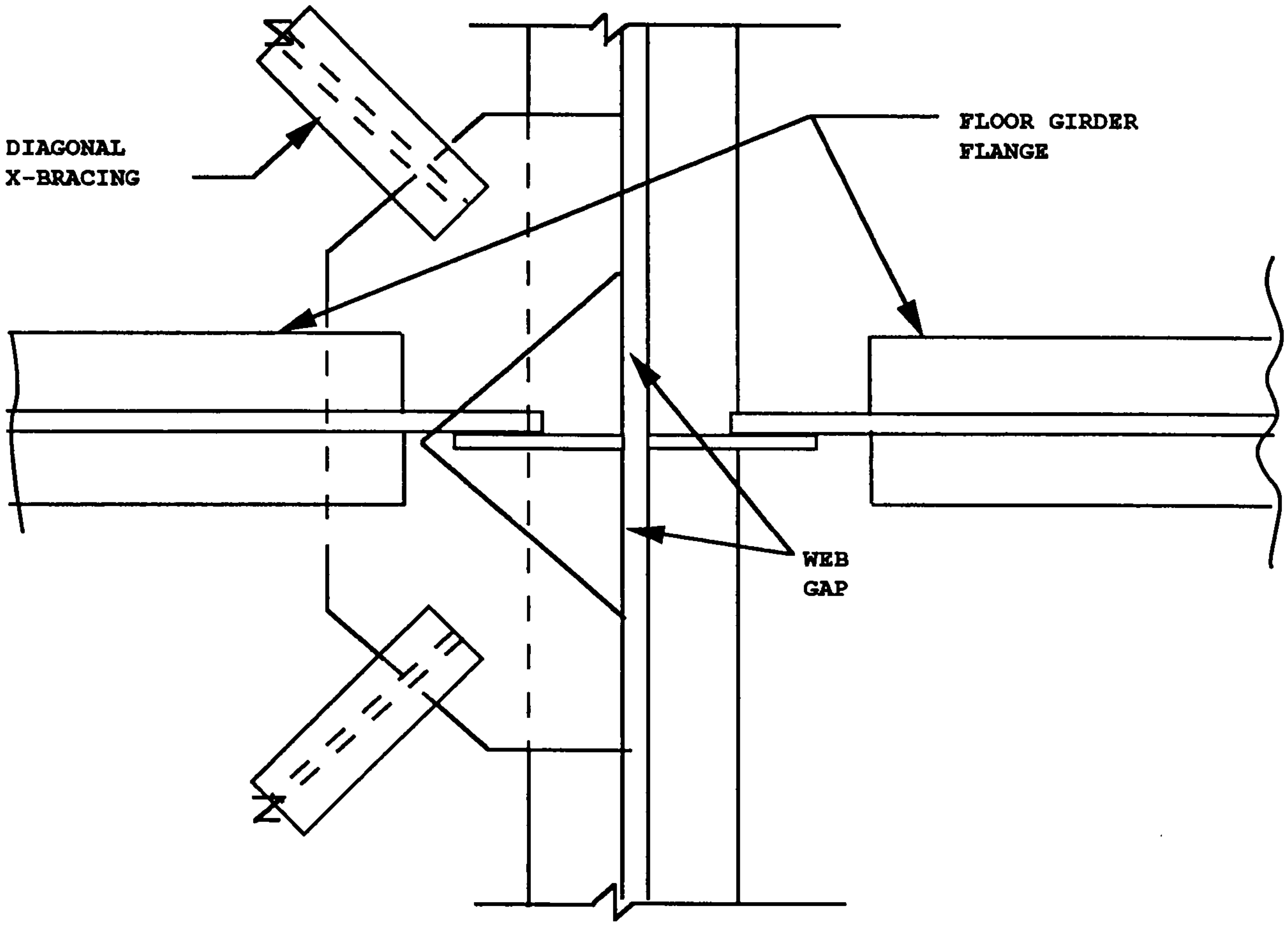

Figure 3.9 - Web Gap at Floor Girder to Main Girder Connection

category E detail(6). With both flanges removed the section modulus of the girder is greatly reduced. This can increase the bending stress in the web plate by 200 or 300 percent at these locations (6). These factors combine to form a location prone to fatigue cracking. The floor beams, therefore, were examined in detail during this study.

CHAPTER IV

INSTRUMENTATION

4.1 Strain Gage Locations

After evaluation of the bridge, specific locations were chosen for application of strain gages. These locations were chosen to determine stresses at fatigue prone details identified during the evaluation. Certain gage locations would also provide information pertaining to the transfer of load from one component to another.

The gage locations were all within the spans defined as one and two on the plans(Figure 4.1). In span one transverse floor girders span between the main girders (Figure 4.2). This situation is typical of all other spans of the bridge, excluding span two. The span length of 135 feet is also fairly typical of the other spans (Figure 4.1). Span one was chosen as the location for study of these typical details due to the ease of access. With a length of 240 feet, span two is the longest of the eight spans. It utilizes floor trusses to support the deck stringers(Figure 4.3). These trusses

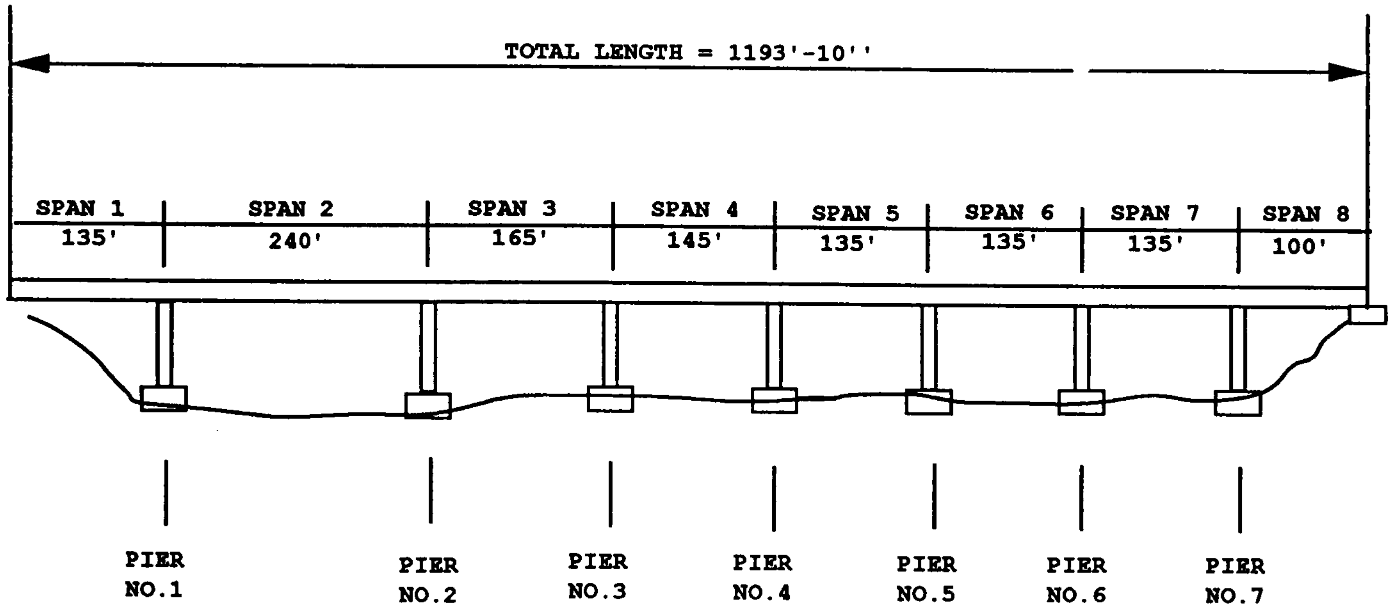

Figure 4.1 - Elevation Looking North

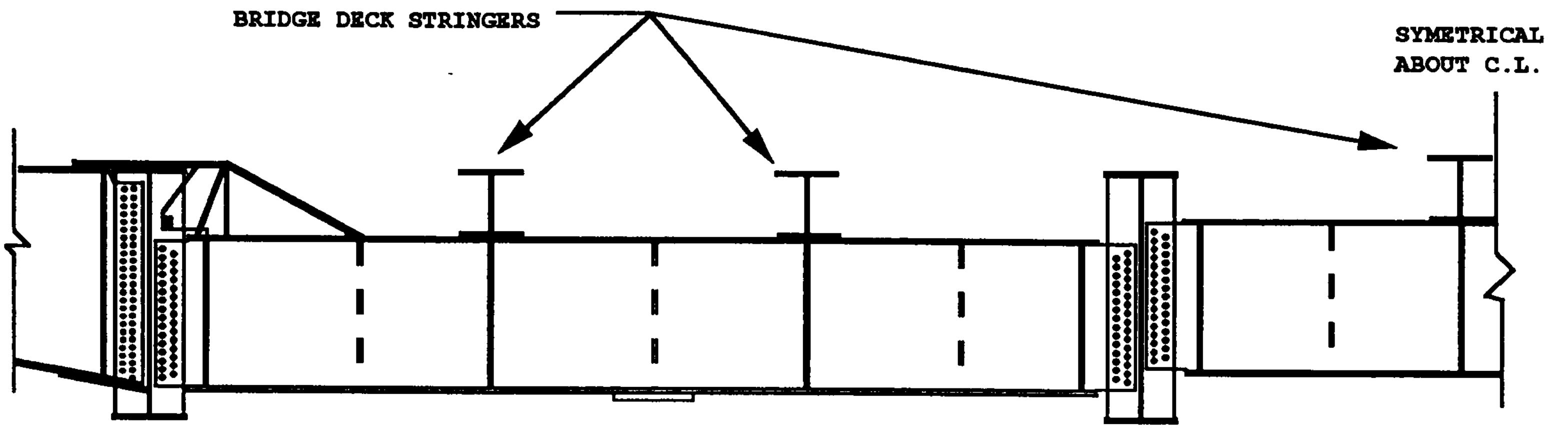

Figure 4.2 - Typical Cross Section at Span Number 1

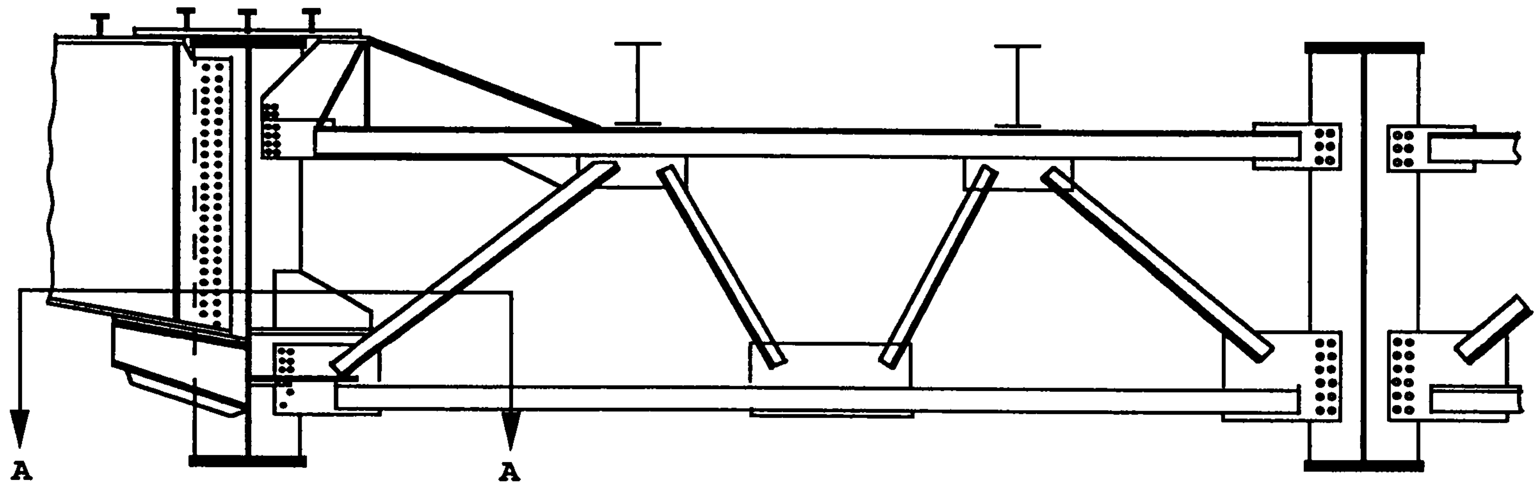

Figure 4.3 - Typical Floor Truss

span between the main girders, as the floor girders do in the other spans. The location of the main girder failure was within span two. Several other locations within this span are identical to the failure location. Four separate locations within this span were extensively instrumented. Typically, twenty three gages were placed at each of these four locations with additional gages added at other particular points of interest at these locations. Gages were also placed on the bottom flanges of the two interior girders to allow for the determination of lateral distribution of load to the four girders.

At each of the locations within span two, the web gap on the exterior girder web was instrumented(Figure 4.4). Three of the four locations received two gages in each of the two web gaps. At the failure location, only the web gap on the opposite side of the vertical stiffener from the fracture was instrumented because of the presence of bolts used to fasten the repair plates in place. A strain gage was located at each side of the web gap(Figure 4.4) to allow for the determination of stresses within the gap. The location of these gages also made it possible to determine if there were any out-of-plane distortions induced over the length of the gap.

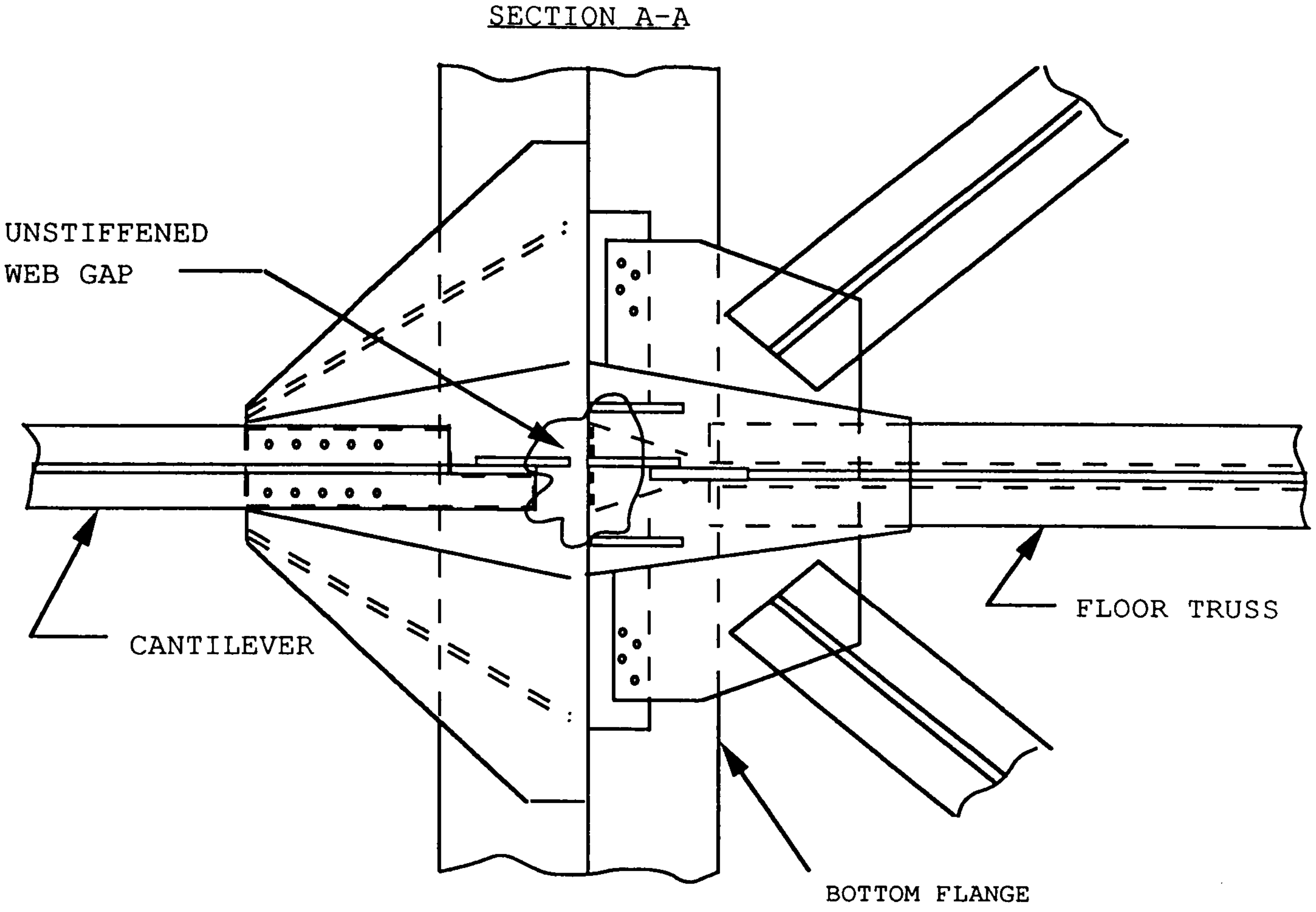

Figure 4.4 - Gages at Exterior Girder Web Gap

If out-of-plane distortions were present, outputs from these gages would be of opposite signs or significantly different. The diagonal X-bracings connected to the lateral gusset plate at this location were also fitted with strain gages. These gages would reveal the contribution these bracing members had to out of plane bending in the web gap.

The floor trusses at each location received identical instrumentation. The bottom chords were fitted with gages at the ends to determine the forces transferred to the girder web. The vertical gusset plate inserted between the double angles that form the bottom chord was also instrumented. The bottom chord angles also received gages at other locations. These gages were attached at the point where the gusset plate that attaches the truss diagonals was inserted between the angles. The locations at which these vertical gusset plates are inserted between the angles represent Category E details. It was desirable to determine stresses here in order to predict the probability of a fatigue crack formation in the gusset plates. The top chords were instrumented directly under the stringers that support the bridge deck. Gages were placed on each side of the top chord to monitor any twisting of the truss due to bending in the stringers. Truss diagonals were also instrumented. This information would be used to determine the load path within the trusses. Figure 4.5 shows the typical layout of gages at a floor truss location. The specific locations of all gages are shown in the appendix.

The top and bottom flanges of the cantilever were each fitted with a strain gage. These gages were at all four locations within span two as well as the test location within span one. These gages would determine if substantial forces were transferred into the girder web from the cantilever.

At the four locations within span two the outside girders received strain gages on the top and bottom flanges. This allowed flexural stresses and the location of the neutral axis to be determined. The interior girders also received gages on their bottom flanges at the cross section where the fracture occurred. Lateral distribution of load to the girders could thereby be measured.

A web gap also existed at the connection of the floor girders to the interior girder. This situation was similar to that which existed prior to the retrofit procedures used in span two. This web gap is not

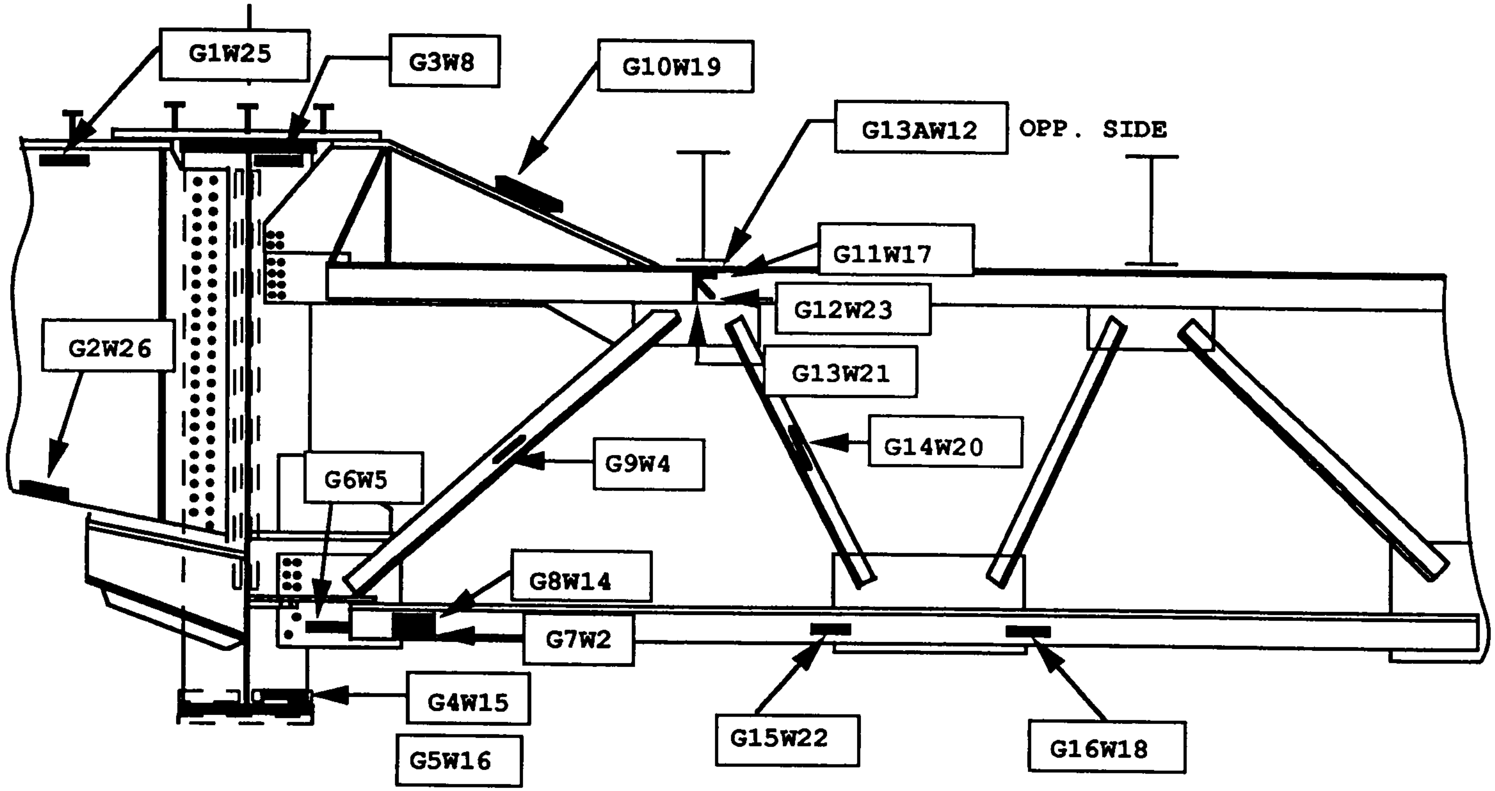

Figure 4.5 - Typical Gage Layout at Span 2

stiffened on the opposite side of the web, as are the retrofitted web gaps of span two. Therefore, it would be more susceptible to out of plane distortion. This web gap received gages identical to those placed in the web gaps located in span two (Figure 4.6). The connection of the floor girders to the main girders was also examined. A possible high stress region exists where the top and bottom flanges are terminated. The termination of the flange web weld at this location creates a Category E detail. Therefore, gages were located on the web in this area at both the top and bottom of the floor girders.

4.2 Procedures

Strain gages were 350 ohm resistance gages manufactured by Micro-Measurements. Gage lengths were either one-quarter or one-eighth inch. The one-eighth inch gages were used in the web gap locations, and the quarter inch gages were used in all other locations. An electric grinder was used to remove paint and mill scale from the gage locations. The locations were then cleaned and strain gages installed as per the manufacturer's instructions.

An Optim MegaDac was used to collect the data from all strain gages. The Megadac was connected to a

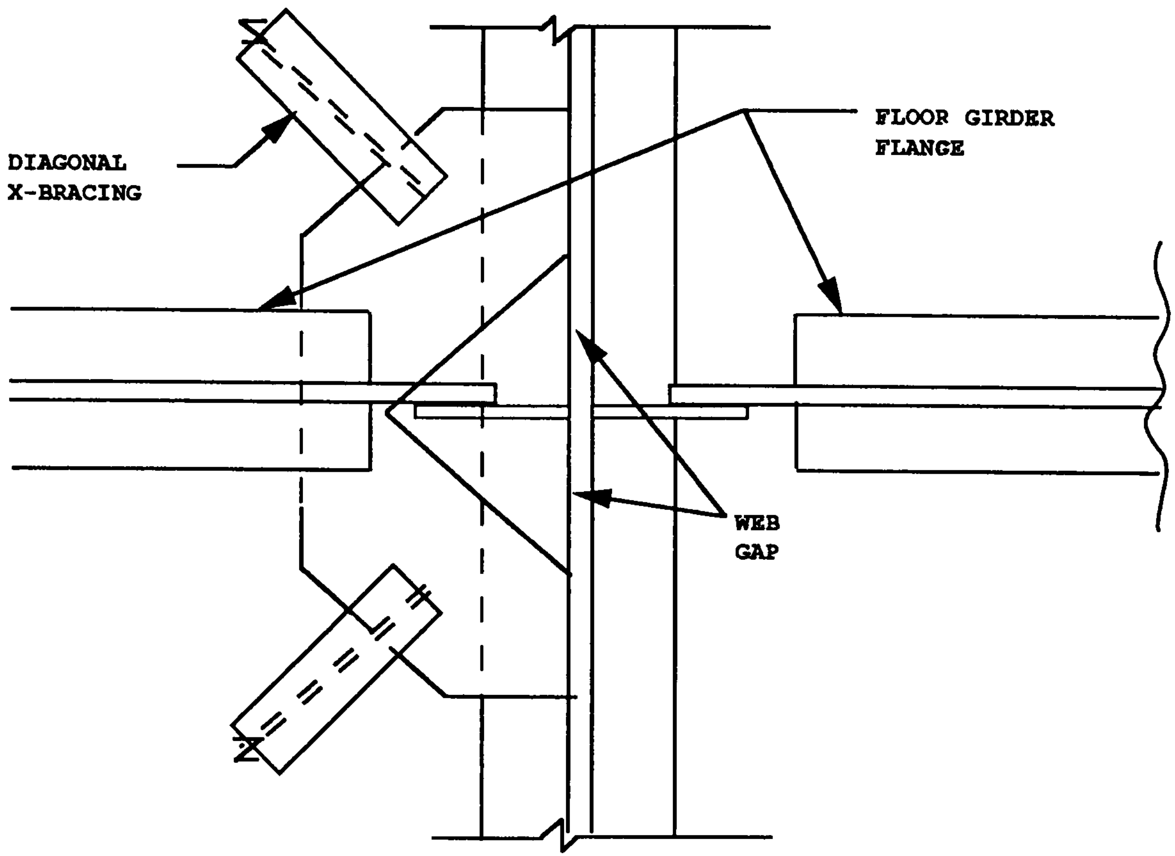

Figure 4.6 - Web Gap at Floor Girder
to Main Girder Connection

personal computer that utilized the TCS 3000 program to control the tests. The TCS 3000 software allowed the research team to check out and balance strain gages prior to each set of tests and observe the readings during tests in the form of graphical plots or digital output. The computer equipment was housed inside a cargo van, which allowed access to the bridge even with a minimum amount of available parking space.

In addition to strain gage data collection, traffic data were also collected during the tests. A video camera was used during several tests to record traffic flow. During other tests manual tallies of truck traffic were recorded. This manual record included direction, lane position, and time relative to the beginning of the test. The video and manual record were analyzed in conjunction with the strain gage data to determine what load condition caused a specific reading at a specific gage location.

CHAPTER V

CONTROLLED LOAD TESTS

5.1 Description of Tests

On August 5, 1993, tests were run using a truck of known weight and axle spacing under controlled traffic conditions. The truck was provided by the Tennessee Department of Transportation. The test truck used was a tandem axle dump truck. The total weight of the truck was 76,760 pounds. The weight on the front axle was 15,260 pounds. The two rear axles combined to support 61,500 pounds. The wheel base of the truck was fourteen feet and eleven inches from the front to the first rear axle and nineteen feet and four inches from front to the second rear axle (Figure 5.1). The width measured seven feet and nine inches from outside to outside of the rear tires. Traffic control was provided by the Knoxville Police Department. It was decided that the tests should be conducted in the early morning hours to minimize the disruption of traffic flow. Tests were begun at 1:00 A.M. and no other traffic was allowed on the bridge when

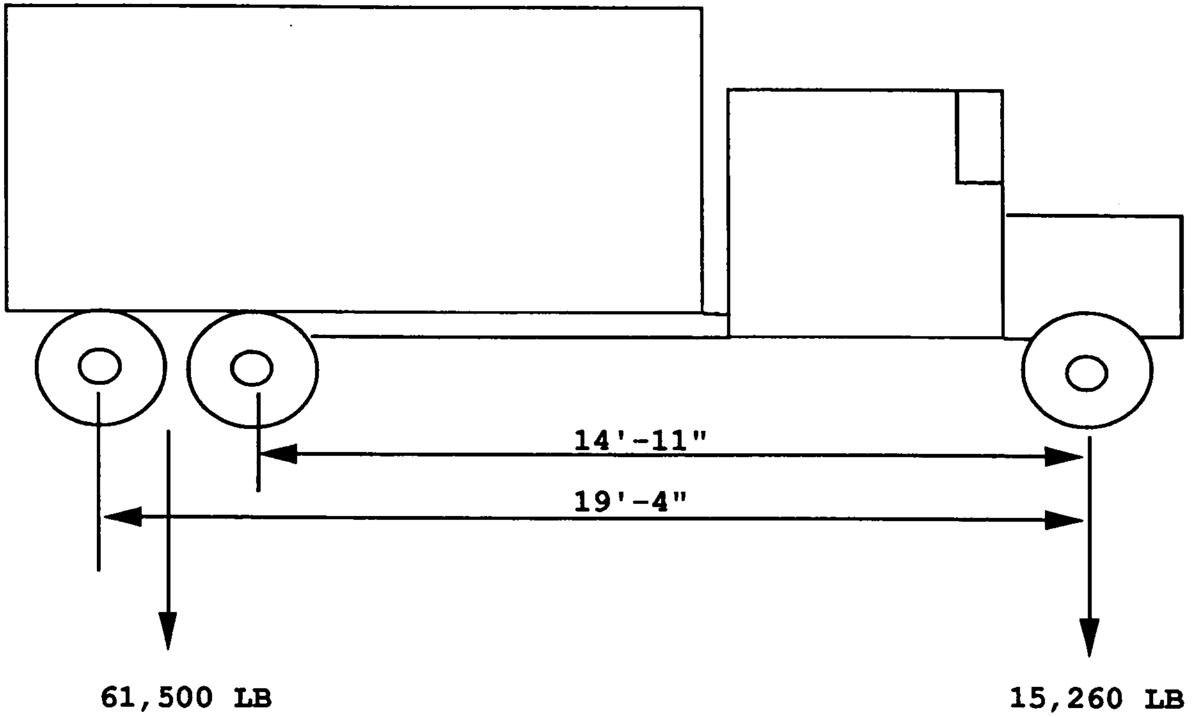

Figure 5.1 - Test Vehicle for Control Load Tests

data were being taken. During all test runs an observer from the research team was in the truck. This was to ensure the driver was in the proper lane and traveling at the proper speed. Radios were utilized to allow communication between the observer, the data collection personnel, and the Knoxville Police Department.

Tests were conducted at crawl speeds to determine the structure's response to a static load moving along the length of the bridge. A constant speed of five miles per hour was maintained. Data collection, for the east bound crawl tests, was begun when the truck reached the west abutment and was stopped when the truck reached the fourth span. All gage locations were in the first and second spans. The effect of the load on these locations was, therefore, negligible by the time the truck reached the fourth span. The west bound tests were begun with the truck at approximately the center of the fourth span and ended when it crossed the west abutment. Crawl test data were taken for all six traffic lanes and for both shoulders. Data were also collected when the truck was returning from the end of each run. This allowed collection of data for two passes in each lane.

Dynamic tests were also conducted with the truck at speeds ranging from fifty to sixty five miles per hour.

The tests with lower speeds were in the east bound lanes due to the proximity of the nearest exit west of the bridge. The truck was only able to obtain a speed of around fifty miles per hour in this relatively short distance. Data were collected for passes with the truck in all six traffic lanes. No dynamic data were taken for the shoulder lanes. The dynamic test data were also collected only when the truck was in the first three spans.

A total of thirty-one gages were monitored during these tests. Gages on the top and bottom flanges of the girders were monitored at locations 1A, 1B, 1C, and 1D(Figure 5.2). Gages on the bottom flanges of the interior two girders, at the cross section where the failure occurred, were also monitored. Due to balancing problems the gage readings were not obtained for the gage on the flange of girder number two. All gages at one location were to be monitored. Location 1D was chosen because all gages were known to be functioning properly at this location prior to the time of the test. Gages at the coped ends of the floor girders in span one were also chosen to be monitored. However, only data from the bottom gage were obtained due to a problem with the top gage just prior to the test.

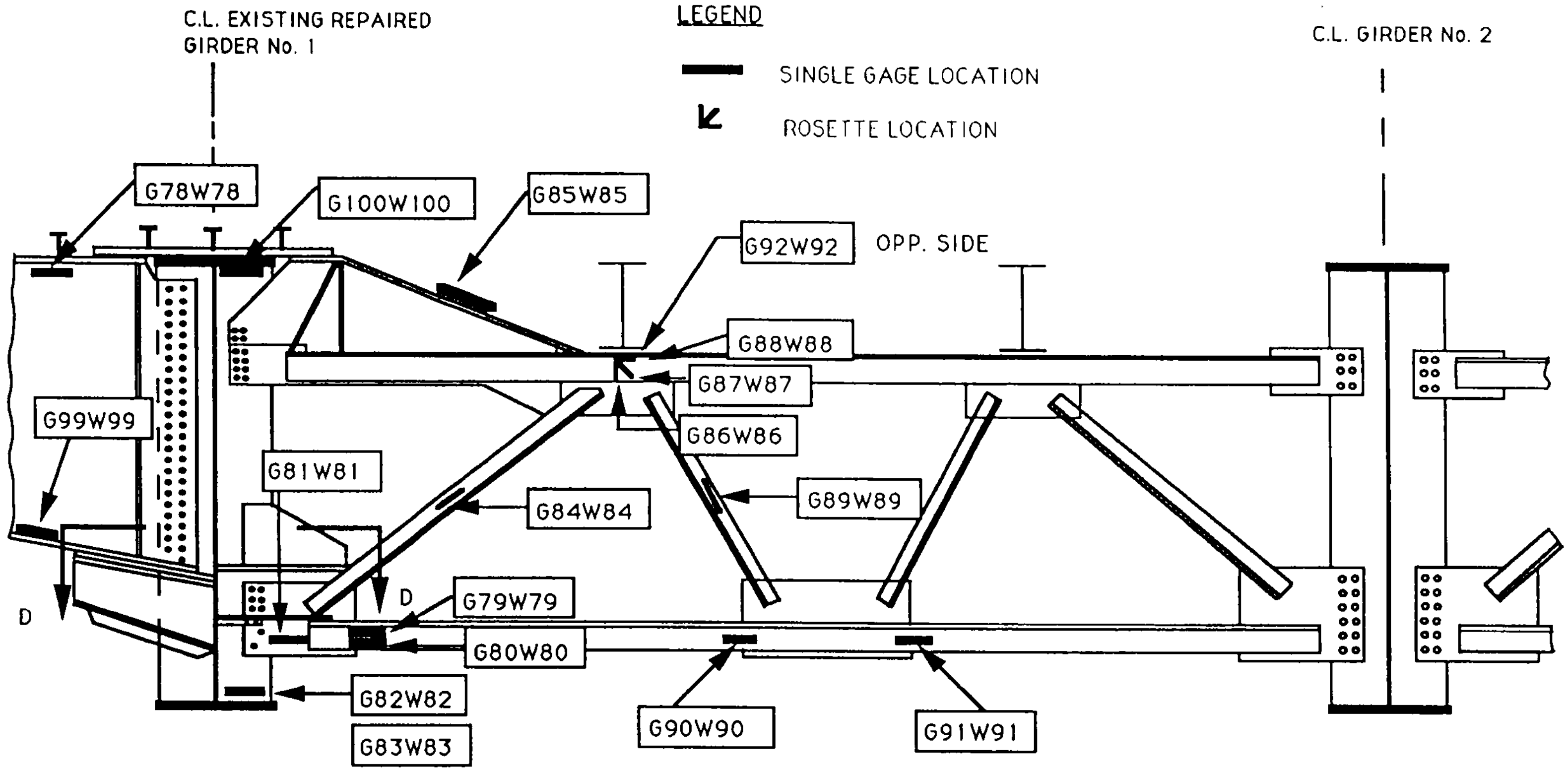

Figure 5.2 - Typical Gage Layout for Controlled Load Tests

CHAPTER VI

TEST RESULTS

6.1 Data Reduction

Strains recorded using the MegaDec and the TCS 3000 software were analyzed using an electronic spreadsheet program. The ability to manipulate large amounts of numerical data quickly and easily made the spreadsheet program ideal for analyzing the controlled load test data. To utilize the spreadsheet, data from TCS 3000 had to be converted to a format compatible with the spreadsheet program. This was done by exporting the data into a Data Interchange File(DIF) within the TCS 3000 program. Once converted into the DIF format the file was transferred to the spreadsheet program where manipulation of the data was possible.

Strain gage readings were taken at a rate of sixty hertz. Although the spreadsheet was capable of handling any of the test files transferred from TCS 3000, the files were quite large and required a great deal of memory. In the opinion of the author and other members of the research team, a lower sample rate adequately reflected the structure's behavior during the controlled load tests. Once the data were transferred to the spreadsheet, it was reduced to reflect a sample rate of ten hertz. This was accomplished by creating a "macro" program within the spreadsheet that automatically deleted the appropriate data from each test file.

The spreadsheet program also allowed the creation of plots for any given gage in any given test(Figure 6.1). These plots made it possible to locate any extraneous data points within a test. These extraneous data points were found in many of the dynamic test files. It is believed that these spikes were caused by outside interference in the gage signal, possibly from two-way radio traffic. Almost all of the invalid points, for any particular test, were at the beginning of the test. A great deal of two-way radio traffic was present at the beginning of each test due to communication between the test truck, the research team, and the police department. These data points were identified and deleted from the test data. The plots also made it possible to determine if a gage had drifted after being balanced. Due to time considerations the gage outputs were not balanced prior to each test. This resulted in the actual zero point

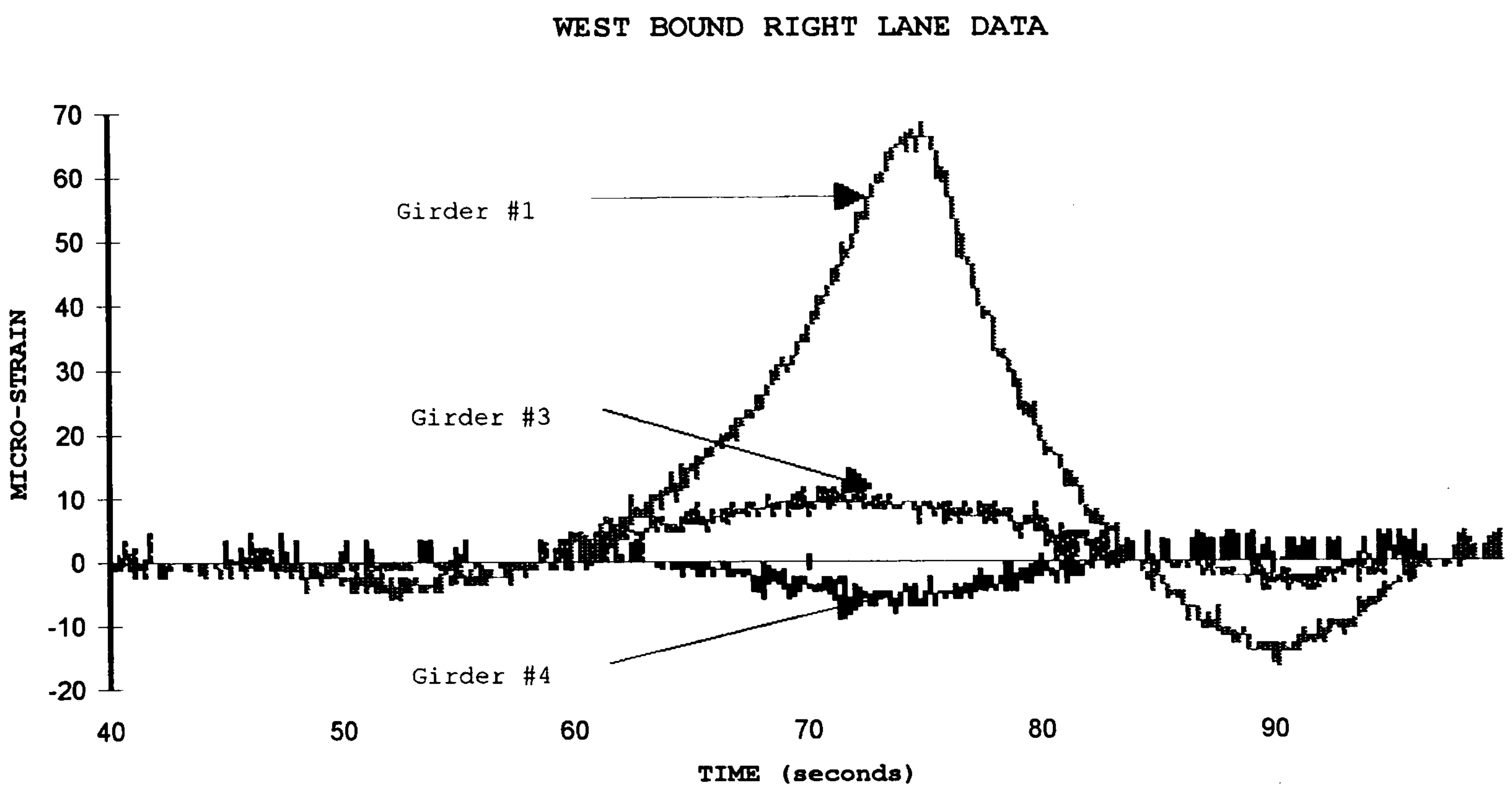

Figure 6.1 - Typical Gage Outputs for Controlled Load Crawl Test Data.

drifting away from the zero axis on the plots. Once identified, the outputs from these gages were corrected for any drift that was present.

Data from each test were reduced, corrected, and analyzed. Maximum stresses at gage locations of interest were determined for each of the test runs. Tables 6.1 and 6.2 show the maximum stresses at the main girder bottom flange for each test. Table 6.1 contains data from the crawl tests and Table 6.2 contains data from the full speed tests. Figure 6.2 shows a typical plot of static verses dynamic test data. Data from two other areas of interest were also examined. These two areas were believed to be locations of high stress and suceptible to fatigue damage. Table 6.3 shows maximum stress ranges at the web gap on girder one. The values for the test runs with the truck in the west bound lanes are given. Test runs with the truck in the east bound lanes had little effect on this location. Table 6.4 shows the maximum stress ranges for the floor beam in the area of the termination of its bottom flange near its connection to the interior girder. These data are from gage number 106(see Appendix B for location).

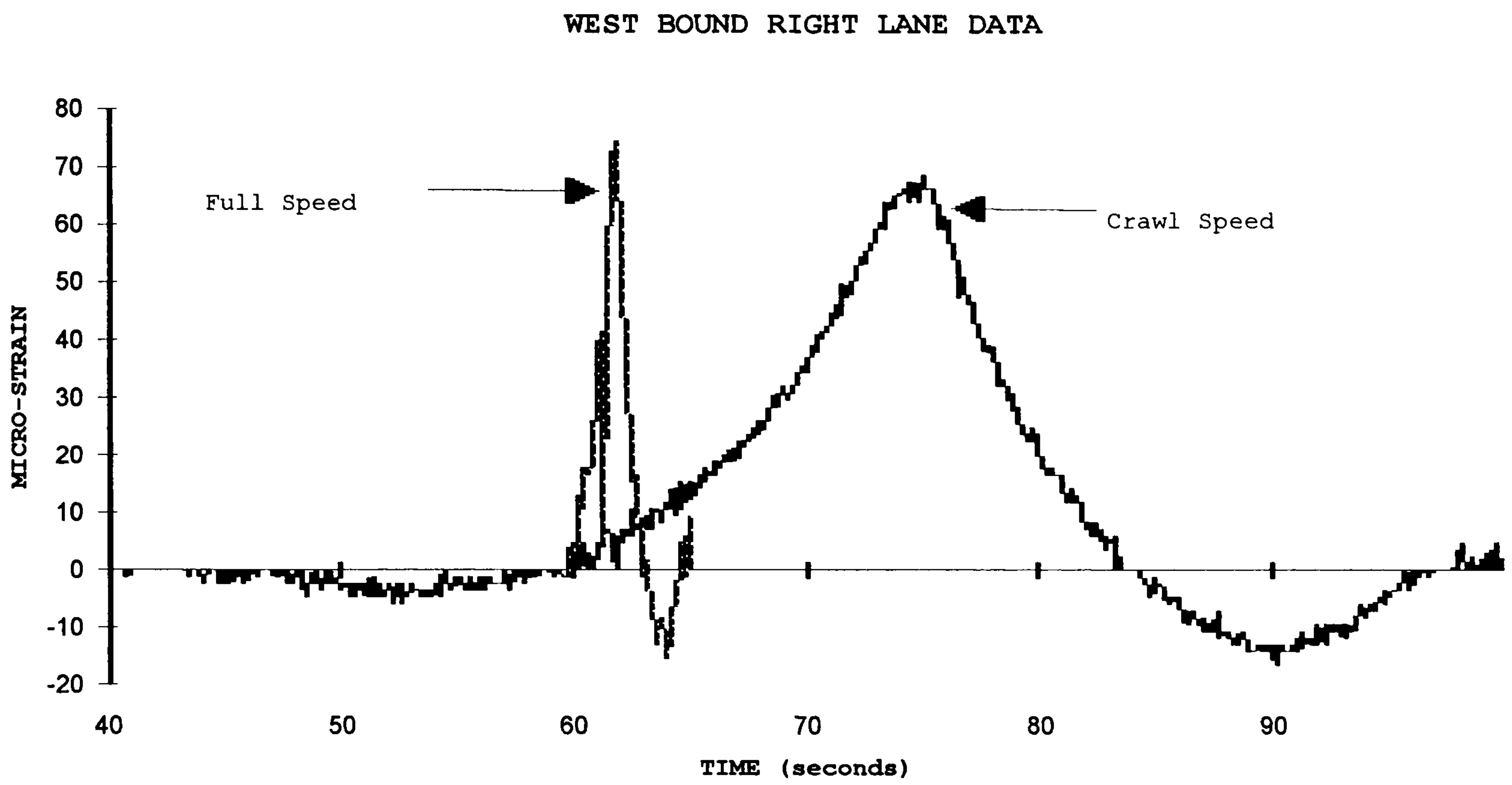

Figure 6.2 - Typical Gage outputs for Controlled Load Crawl and Full Speed Test Data.

Table 6.1 - Maximum Main Girder Stresses for Crawl Tests

MAX BOTTOM FLANGE STRESSES FOR CRAWL TESTS(PSI)					
		EAST BOUND			
GIRDER #		SHOULDER	RIGHT LANE	MIDDLE LANE	LEFT LANE
1	POS	103	206	172	206
	NEG	-412	-172	-69	-240
	RANGE	515	378	240	446
3	POS	618	893	1374	1442
	NEG	-481	-309	-309	-412
	RANGE	1099	1202	1683	1854
4	POS	2541	2473	1545	790
	NEG	-790	-549	-481	-481
	RANGE	3331	3022	2026	1271

		WEST BOUND			
GIRDER #		SHOULDER	RIGHT LANE	MIDDLE LANE	LEFT LANE
1	POS	2095	1992	1339	756
	NEG	-618	-481	-412	-343
	RANGE	2713	2473	1751	1099
3	POS	240	343	549	790
	NEG	-172	-137	-206	-206
	RANGE	412	481	756	996
4	POS	206	137	172	412
	NEG	-412	-240	-103	-137
	RANGE	618	378	275	549

Table 6.2 - Maximum Main Girder Stresses for Dynamic Tests

MAX BOTTOM FLANGE STRESSES FOR DYNAMIC TESTS(PSI)					
		EAST BOUND			
GIRDER #		SHOULDER	RIGHT LANE	MIDDLE LANE	LEFT LANE
1	POS	N/A	378	172	309
	NEG	N/A	-172	-172	-103
	RANGE	N/A	549	343	412
3	POS	N/A	925	1477	1923
	NEG	N/A	-414	-343	-240
	RANGE	N/A	1339	1820	2164
4	POS	N/A	2438	1545	996
	NEG	N/A	-756	-584	-378
	RANGE	N/A	3194	2129	1374

		WEST BOUND			
GIRDER #		SHOULDER	RIGHT LANE	MIDDLE LANE	LEFT LANE
1	POS	N/A	2164	1271	824
	NEG	N/A	-446	-584	-343
	RANGE	N/A	2610	1854	1168
3	POS	N/A	197	446	721
	NEG	N/A	-231	-206	-206
	RANGE	N/A	428	652	927
4	POS	N/A	240	137	343
	NEG	N/A	-275	-172	-240
	RANGE	N/A	515	309	584

Table 6.3 - Maximum Stress Ranges at web Gap on Girder 1

TRUCK POSITION	MAXIMUM STRESS RANGE (PSI)	
	STATIC	DYNAMIC
WEST BOUND LEFT LANE	2095	2335
WEST BOUND MIDDLE LANE	3125	3434
WEST BOUND RIGHT LANE	3846	4155

Table 6.4 - Maximum Stress Ranges at Floor Beam bottom Flange Termination

TRUCK POSITION	STRESS RANGE (PSI)	
	STATIC	DYNAMIC
EAST BOUND SHOULDER	2267	N/A
EAST BOUND RIGHT LANE	1854	2026
EAST BOUND MIDDLE LANE	1133	1820
EAST BOUND LEFT LANE	3091	4121
WEST BOUND LEFT LANE	756	1477
WEST BOUND MIDDLE LANE	962	1133
WEST BOUND RIGHT LANE	1580	1820
WEST BOUND SHOULDER	1923	N/A

CHAPTER VII

ANALYSIS OF DATA

7.1 Introduction

It has been shown by several other researchers that the approximations commonly used to predict stresses in members for design produce conservative results(17,21,23,24). The Holston River Bridge project provided an excellent opportunity to measure the response of an actual structure to applied loads. Data collected during the controlled load tests provide a means of evaluating the accuracy of assumptions and simplifications made during the design of this and other bridges. The data were analyzed and compared with results obtained using analytical methods developed by other researchers(5) in an attempt to verify the results of these methods. The actual measured responses were also compared to values obtained using AASHTO values.

7.2 Lateral Load Distribution

Deatherage (5) attempted to provide engineers with a better means of evaluating load distributions for beam-slab bridges. He extended the Guyon-Massonnet theory and developed a series of influence coefficients which can be used to predict the effect of a load applied laterally at any point on the cross section of a bridge. The values of these influence coefficients depend on a flexural parameter, θ, and a torsional parameter, α, which are specific to the particular structure being evaluated. Curves representing influence coefficients verses the relative lateral location of loads, for the Holston River Bridge were developed(Figure 7.1 and 7.2). From these curves distribution coefficients for interior and exterior girders for test trucks in all six lanes were calculated.

AASHTO uses a distribution factor based on the girder spacing divided by a constant for a particular type of structure. An AASHTO distribution coefficient obtained by dividing the girder spacing by 5.5 was calculated.

By superimposing measured maximum stresses for each pass of the test truck, maximum stresses equivalent to those that would be produced with a truck in all six

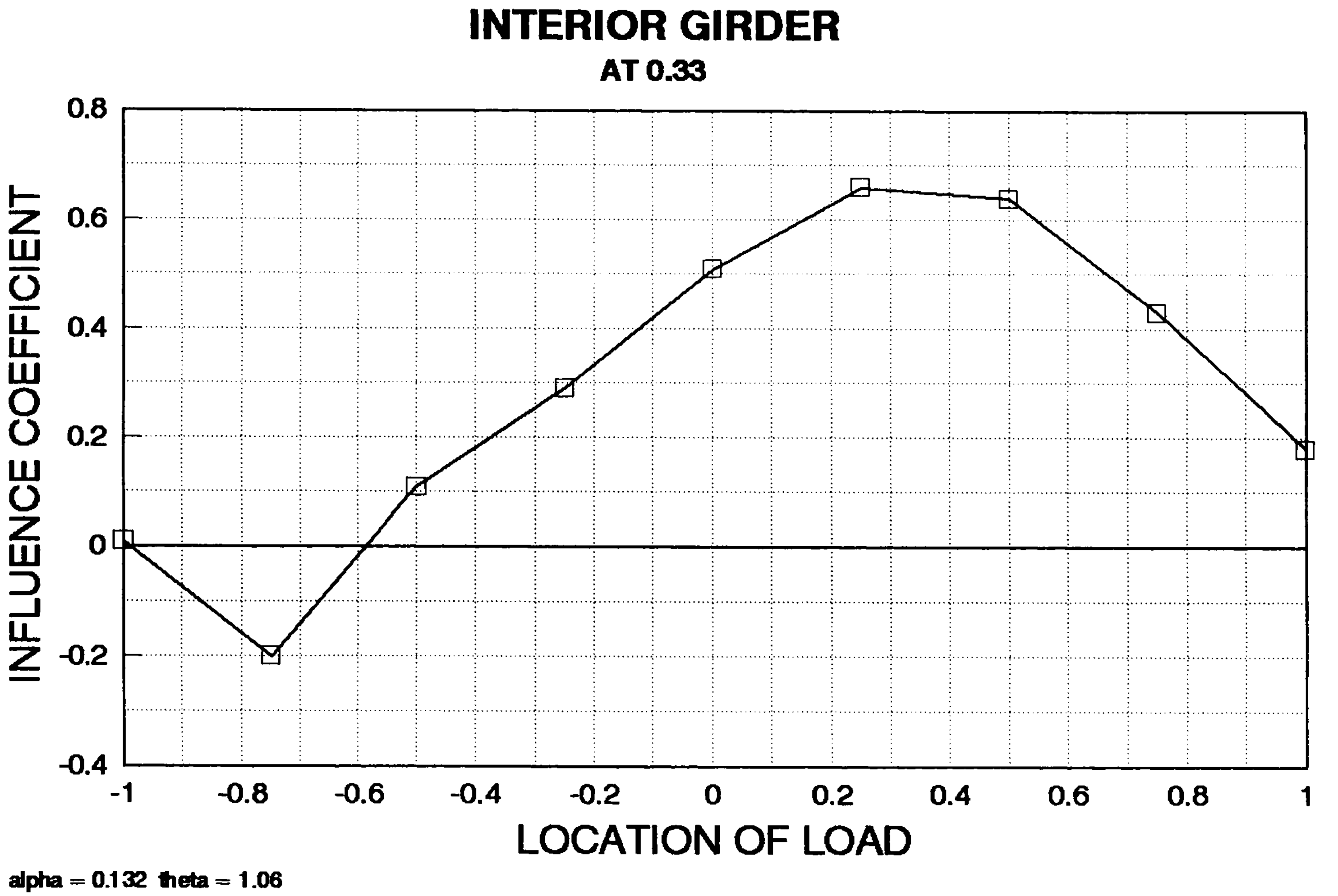

Figure 7.1 - Influence Coefficients for Interior Girder

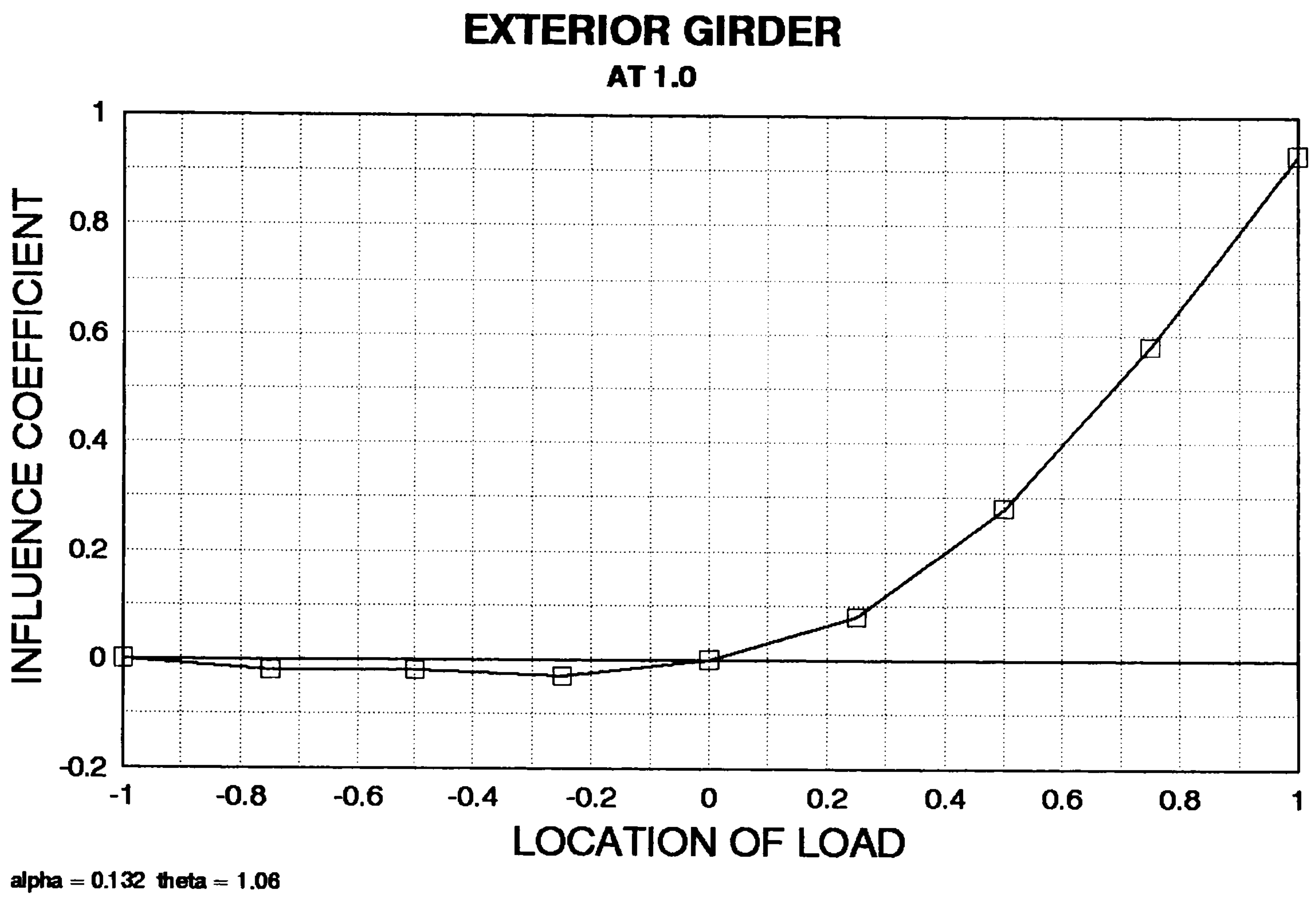

Figure 7.2 - Influence Coefficients for Exterior Girder

lanes could be obtained for each girder. These stresses were used to determine an actual distribution factor. This distribution factor was then compared to both calculated distribution factors.

Computer models for exterior and interior girders were developed using GTSTRUDL. With the aid of these models and the calculated distribution factors, moments for each girder were determined at the bottom flange strain gage locations. The stresses for the bottom flange of each girder were then calculated using the section properties at strain gage locations. These stresses were compared to the actual measured stresses at the bottom flanges of the main girders.

Table 7.1 summarizes the distribution factors and stresses from both methods and actual measurements. The appendix of this thesis shows the calculations of flexural and torsional parameters , distribution factors, and stresses.

7.3 Dynamic Impact Factors

Another important variable in determining design forces in bridge members is the dynamic impact factor. Other researchers have found that the AASHTO allowance

Table 7.1 - Calculated and Measured Maximum Stresses

GIRDER NUMBER	AASHTO		CALCULATED		MEASURED	
	DISTRIBUTION FACTOR	MAX STRESS*	DISTRIBUTION FACTOR	MAX STRESS*	DISTRIBUTION FACTOR	MAX STRESS*
3(interior)**	4.72	11.50	3.38	8.22	2.28	5.39
1(exterior)	4.72	11.50	2.36	5.74	1.92	4.67
4(exterior)	4.72	11.50	2.36	5.74	2.27	5.53

* All Stresses Given in KSI

**Stesses were not measured for interior girder #2 for dynamic impact is usually higher than that measured during tests(15)(23)(25). AASHTO uses the value of

$$I = 50/(L+125)$$

for the increase in live load due to dynamic impact. This equation takes the span length as its only variable. However, research has shown that the dynamic impact factor is directly controlled by road surface roughness(15,23,25).

During the controlled load tests on the Holston River Bridge, data were taken for both crawl and full speed tests. Comparing the maximum stresses in the two sets of tests allowed the determination of an actual impact factor. Impact factors were calculated for three loations on the Bridge. These loations included the bottom flange of the main girders in span two, the web gap on girder one in span two, and the floor beam in span one. The test runs which produced maximum stresses below 1000 pounds per square inch were not included in the calculations due to the more pronounced effect of outside interference on these readings. These factors were then compared to AASHTO's value of 50/(L+125). Tables 7.2, 7.3, and, 7.4 show the dynamic impact values for each location along with the AASHTO value.

Table 7.2 - Dynamic Impact Factors for Girders

TEST RUN	GIRDER #	MAX STRESS RANGE STATIC	MAX STRESS RANGE DYNAMIC	IMPACT FACTOR
RIGHT LANE E. BOUND	1	378	549	N/A*
	3	1202	1339	1.11
	4	3022	3194	1.06
MIDDLE LANE E. BOUND	1	240	343	N/A*
	3	1683	1820	1.08
	4	2026	2129	1.05
LEFT LANE E. BOUND	1	446	412	N/A*
	3	1854	2164	1.17
	4	1271	1374	1.08
RIGHT LANE W. BOUND	1	2473	2610	1.06
	3	481	428	N/A*
	4	378	515	N/A*
MIDDLE LANE W. BOUND	1	1751	1855	1.06
	3	756	652	N/A*
	4	275	309	N/A*
LEFT LANE W. BOUND	1	1099	1168	1.06
	3	996	927	N/A*
	4	549	584	N/A*

*Run With Stress Range Below 1000psi

MAX MEASURED= 1.17
AASHTO = 1.14

Table 7.3 - Dynamic Impact Factors for Web Gap on Girder Number 1

TRUCK POSITION	MAXIMUM STRESS RANGE (PSI)		IMPACT FACTOR
	STATIC	DYNAMIC	
WEST BOUND LEFT LANE	2095	2335	1.11
WEST BOUND MIDDLE LANE	3125	3434	1.10
WEST BOUND RIGHT LANE	3846	4155	1.08

AASHTO= 1.14

Table 7.4 - Dynamic Impact Factors for Floor Beam

TRUCK POSITION	STRESS RANGE (PSI)		IMPACT FACTOR
	STATIC	DYNAMIC	
EAST BOUND SHOULDER	2267	N/A	N/A
EAST BOUND RIGHT LANE	1854	2026	1.09
EAST BOUND MIDDLE LANE	1133	1820	1.61
EAST BOUND LEFT LANE	3091	4121	1.33
WEST BOUND LEFT LANE	756	1477	N/A
WEST BOUND MIDDLE LANE	962	1133	1.18
WEST BOUND RIGHT LANE	1580	1820	1.15
WEST BOUND SHOULDER	1923	N/A	N/A

AASHTO = 1.19*

*Value Calculated Using L= 135'=Length of Span 1

CHAPTER VIII

CONCLUSIONS

AASHTO provides a simple method for determining the lateral distribution of loads to a particular girder. This method, however, has been shown to produce very conservative results in the case of the Holston River Bridge as well as others(5,17,21,23). The AASHTO factors led to the calculation of stresses that were in excess of two times the actual measured stresses for both interior and exterior main girders. While sophisticated computer modeling techniques can potentially provide much more accurate results, the time involved and level of expertise required may outweigh the benefits of a more precise solution. The need for a methodology which quickly and accurately predicts the portion of applied load carried by a single member is evident. Even when a more sophisticated computer model is to be used, a method accurate enough to verify its results is useful. Deatherage attempted to provide such a method. This method accounts for both bending and torsional stiffness in laterally distributing the loads. When applied to the Holston River Bridge this method produced results which, while still conservative, were less conservative than AASHTO for both the interior and exterior girders. The method was much more accurate for the exterior girders and less so for the interior. However, this method does provide a simple and quick procedure for determining the appropriate amount of applied loads to assign to longitudinal members.

The dynamic impact factor used by AASHTO has been shown by several researchers to be higher than that actually measured in some cases(15,23,25). The AASHTO equation for the dynamic impact factor takes only one variable into consideration, span length. A review of the recent research on the effect of variables on the dynamic impact factor shows that this is not the controlling factor. Instead, roadway roughness has been found to be the controlling factor.

The values measured on the Holston River Bridge varied depending on the location being considered. The measured impact factors for the main girders in span two compared relatively well with the AASHTO value. Although one test run produced a value above the AASHTO value, the measured values were consistently lower than calculated.

The measured values at the floor beam in span one, however, do not compare well with the AASHTO value. The AASHTO value to be used for this location was calculated using the span length of the main girders in span one(135'), as is believed to be normal practice. There was evidence that this value when applied to the floor beams is unconservative.

LIST OF REFERENCES

LIST OF REFERENCES

(1) American Association of State Highway and Transportation Officials, Standard Specification for Highway Bridges, 13th Edition, 1983.

(2) American Institute of Steel Construction, Manual of Steel Construction, 9th Edition, 1989.

(3) Bakht, B., Jaeger, L.G., Bridge Analysis Simplified, McGraw-Hill, 1985.

(4) Chan, T.H., O'Connor, C., "Wheel Loads From Highway Bridge Strains: Field Studies," Journal of Structural Engineering, Vol 116 No. 7,July 1990, pp175-71.

(5) Deatherage, J.H., "Investigation of Variables Affecting Beam-Slab Bridge Load Capacity," Ph. D. Dissertation, University of Tennessee at Knoxville, June 1987.

(6) Fisher, J.W., "Fatigue Cracking in Steel Bridges and Techniques for Retrofitting," Center for Advanced Technology for Large Structural Systems, 1993.

(7) Fisher, J.W., Nussbaumer, A., Keating, P.B., Yen, B.T., "Resistance of Welded Details Under Variable Amplitude Long-Life Fatigue Loading," National Cooperative Highway Research Program Report 354, 1993.

(8) Fisher, J.W., Jin, J., Wagner, D.C., Yen, B.T., "Distortion-Induced Fatigue Cracking in Steel Bridges," National Cooperative Highway Research Program Report336, Transportation Research Board, December 1990.

(9) Fisher, J.W., Yen, B.T., Wang, D., "Fatigue Cracking of Steel Bridge Structures," Volume II: A Commentary and Guide for Design, Evaluation, and Investigation of Cracking, FHWA-RD-89-167, March 1990.

(10) Fisher, J.W., "Executive Summary: Fatigue Cracking in Steel Bridge Structures," ATLSS Report No. 89-03, July 1989.

(11) Fisher, J.W., Yen, B.T., Wagner, D.C., "Review of Field Measurements for Distortion Induced Fatigue Cracking in Steel Bridges," Transportation Research Board, Washington, D.C., 1987.

(12) Fisher, J.W., Mertz, D.R., 'Retrofitting Steel Bridges to Extend Their Fatigue Lives," The 1985 International Engineering Symposium on Structural Steel, Chicago, IL., May 1985.

(13) Fisher, J.W., Fatigue and Fracture in Steel Bridges, Case Studies, John Wiley and Sons, 1984, pp 61-76.

(14) Fisher, J.W., Barthelemy, B.M/, Mertz, D.R., Edinger, J.A., "Fatigue Behavior of Full Scale Welded Bridge Attachments," National Cooperative Highway Research Program Report 227, Transportation Research Board, November 1980.

(15) Ghosn, M., Moses, F., Gobieski, J., "Evaluation of Steel Bridges Using In-Service Testing," Transportation Research Record 1072, Transportation Research Board, Washington, D.C., 1986.

(16) Gupta, A.K., "Field Tests of a Continuos Twin Girder Steel Bridge," University of Texas at Austin, May 1981.

(17) Hays, C.O., Sessions, L.M., Berry, A.J., "Further Studies on Lateral Load Distribution Using a Finite Element Method," Transportation Research Record 1072, Transportation Research Board, Washington, D.C., 1986.

(18) Keating, P.B., Fisher, J.W., "Evaluation of Fatigue Tests and Design Criteria on Welded Details," National Cooperative Research Program Report 286, Transportation Research Board, December 1986.

(19) Kulicki, J.M., Murphy, R.E., Mertz, D.R., Fisher, J.W., "Fatigue Cracking on I-79 Bridges in West Virginia," Fritz Engineering Laboratory, Lehigh University, 1986

(20) Lee, J.J., Yen, B.T., Fisher, J.W.,Castiglioni, C, "Forces and Displacements of Diaphragm Members in a Multigirder Steel Bridge," Second Annual International Bridge Conference, Pittsburgh, PA, June 1985.

(21) Moore, M., Strand, K.A., Grubb, M.A., Cayes, L.R., "Wheel-Load Distribution Results from AISI-FHWA Model Bridge Study," Transportation Research Record 1275, Transportation Research Board, Washington, D.C., 1990.

(22) Moses, F., Verma, D., "Load Capacity Evaluation of Existing Bridges," National Cooperative Highway Research Program Report 301, Transportation Research Board, Washington, D.C., 1987.

(23) Moses, F., Ghosn, M., Snyder, R.E., "Application of Load Spectra to Bridge Rating," Transportation Research Record 950, Transportation Research Board, Washington, D.C., 1984.

(24) Nowak, A.S., Nassif, H., Frank, K.H., "Fatigue Load Spectra for Steel Girder Bridge," Transportation Research board, Washington, D.C., 1993.

(25) Nowak, A.S., Hong, Y-K, Hwang, E-S, "Modeling Live Load and Dynamic Load for Bridges," Transportation Research Record 1290, Transportation Research Board, Washington, D.C., 1991.

(26) Ozbek, A., "Lateral Load Distribution in Beam - Slab Highway Bridges," Masters Thesis, University of Tennessee, June 1987.

APPENDICES

APPENDIX A

SAMPLE CALCULATIONS

CALCULATE THE LOAD DISTRIBUTION PARAMETERS FOR THE HOLSTON RIVER BRIDGE.

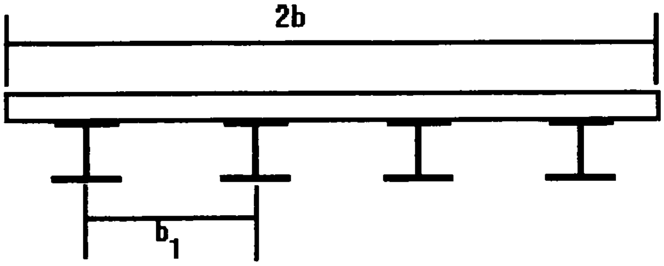

CROSS SECTION - HOLSTON RIVER BRIDGE

GEOMETRIC PROPERTIES:

Length of Span: L = 240 feet

Deck Thickness: h = 7.5 inches

Compressive Strength of Concrete: f'_c = 3000 psi

Modulus of Elasticity of Concrete:

$E_C = 57(f'_C)^{0.5} = 57(3000)^{0.5} = 3122$ ksi

Modulus of Elasticity of Steel: E_s = 29000 ksi

Modular Ratio: $n = E_s/E_c = 29/3.12 = 9.29$

TRANSFORMED SECTION:

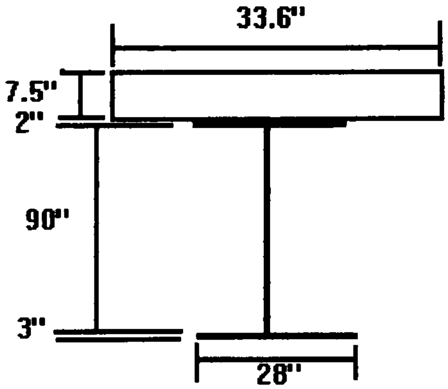

$b_e = b/n = 26(12)/9.29 = 33.6"$

Locate Neutral Axis of Transformed Section:

$$X = \frac{\Sigma xA}{\Sigma A} = \frac{98.75(252)+94(56)+48(33.75)+1.5(84)}{252+56+33.75+84}$$

X = 74.91" from bottom of section

Moment of Inertia of Transformed Section:

$$I_{slab} = 28(7.5)^3/12 + 252(23.84)^2 = 144,207$$
$$I_{top\ flg} = 28(2)^3/12 + 56(19.09)^2 = 20,427$$
$$I_w = 0.375(90)^3/12 + 33.75(26.91)^2 = 47,221$$
$$I_{bot\ flg} = 28(3)^3/12 + 84(73.41)^2 = 452,741$$

$$I = \Sigma I = 144,207+20,427+47,221+452,741 = 664,597 in^4$$

Moment of Inertia of Unit Width of Deck:

$$I_D = 12(7.5)^3/7.5 = 422 \ in^4$$

Girder Spacing: b_1 = 26 feet = 312 inches

Width of Equivalent Bridge: $2b = 3b_1 + 2(b_1/2)$
$= 3(26)+26 = 104$ feet

b = 52 feet

Torsional Constant for Transformed Section: J_G

$$J_G = \Sigma(J_{beam} + J_{deck})$$
$$J_{bm} = 0.28At_f^2 = 0.28(173.75)(3)^2 = 437.85 \text{ in}^4$$
$$J_d = (b_t - 0.63h)h^3/3 = [33.6-0.63(7.5)](7.5)^3/3$$
$$= 4061 \text{ in}^4$$
$$J_G = 437.85 + 4061 = 4499 \text{ in}^4$$

Calculate Θ:

$$B_G = E_G I_G = 29x10^6 \ (664{,}597) = 1.93x10^{13}$$
$$B_D = E_D I_D = 3.122x10^6(422) = 1.317x10^9$$
$$\rho_G = B_G/b_1 = 1.93x10^{13}/312 = 61.86x10^9$$
$$\rho_D = B_D/W \quad \text{(W=Unit Width=12in)}$$
$$= 1.317x10^9/12 = 10.98x10^7$$

$$\Theta = (b/L)(\rho_G/\rho_D)^{0.25}$$
$$= (52/240)(61.86x10^9/10.98x10^7)^{0.25}$$
$$= 1.06$$

Calculate α:

$$C_G = J_G G_G$$
$$G_G = E/[2(1+v)] = 29(10^6)/[2(1+0.3)] = 11.15x10^6 \text{psi}$$
$$C_G = 4499(11.15x10^6) = 50{,}164x10^6$$
$$Y_G = C_G/b1 = 50{,}164x10^6/312 = 160.8x10^6$$
$$C_D = J_D G_D$$
$$G_D = E_c/2 = 3.122x10^6/2 = 1.56x10^6$$
$$C_D = 4061(1.56x10^6) = 6335x10^6$$
$$Y_D = C_D/W = 6335x10^6/12 = 528x10^6$$

$\alpha = Y_G + Y_D / [2(\rho_G \rho_D) 0.5]$

$= 160.8\text{x}10^6 + 528\text{x}10^6 / [2(61.86\text{x}10^9) 10.98\text{x}10^7)]$

$= 0.132$

CALCULATION OF STRESSES USING DEATHERAGE'S INFLUENCE COEFFICIENTS:

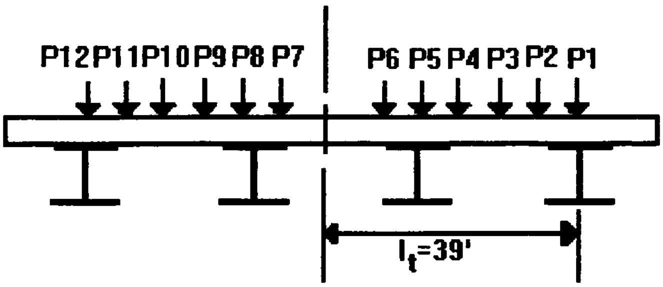

Test Truck Weight = 76760 lbs

P = 76760/2 = 38380 lbs

Relative Location of Load Values for use with Influence Coefficient Curves:

$l_1/l_t = 38/39 = 0.97$

$l_2/l_t = 31/39 = 0.79$

$l_3/l_t = 26/39 = 0.67$

$l_4/l_t = 19/39 = 0.49$

$l_5/l_t = 14/39 = 0.36$

$l_6/l_t = 7/39 = 0.18$

$l_7/l_t = -l_6/lt = -0.18$

$l_8/l_t = -l_5/l_t = -0.36$

$l_9/l_t = -l_4/l_t = -0.49$

$l_{10}/l_t = -l_3/l_t = -0.67$

$l_{11}/l_t = -l_2/l_t = -0.79$

$l_{12}/l_t = -l_1/l_t = -0.97$

Values from Coefficient Curves for Exterior Girder:

$P_{G1} = 0.89P$	$P_{G7} = -0.01P$
$P_{G2} = 0.62P$	$P_{G8} = -0.03P$
$P_{G3} = 0.47P$	$P_{G9} = -0.02P$
$P_{G4} = 0.26P$	$P_{G10} = -0.02P$
$P_{G5} = 0.16P$	$P_{G11} = -0.02P$
$P_{G6} = 0.06P$	$P_{G12} = 0P$

$\Sigma P_{Gn} = 2.36P = 2.36(38,380)(1/1000) = 90.58$ kips

M = 3763 K-FT (From GTSTRUDL)

Stress at top side of bottom flange:

$f = Mc/I = 3763(12)(75.63)/594520 = 5.74$ ksi

APPENDIX B

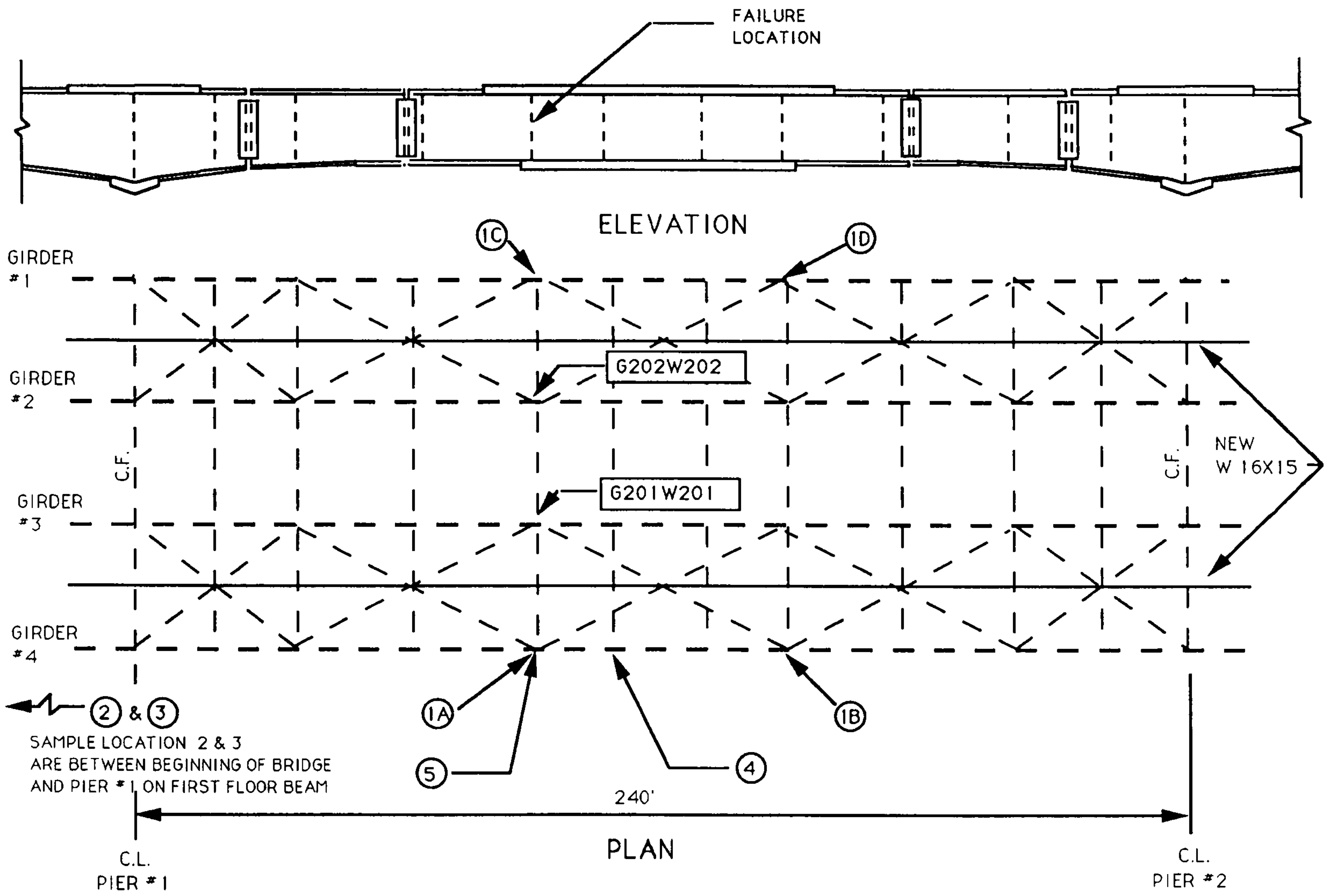

DATA SAMPLE LOCATIONS

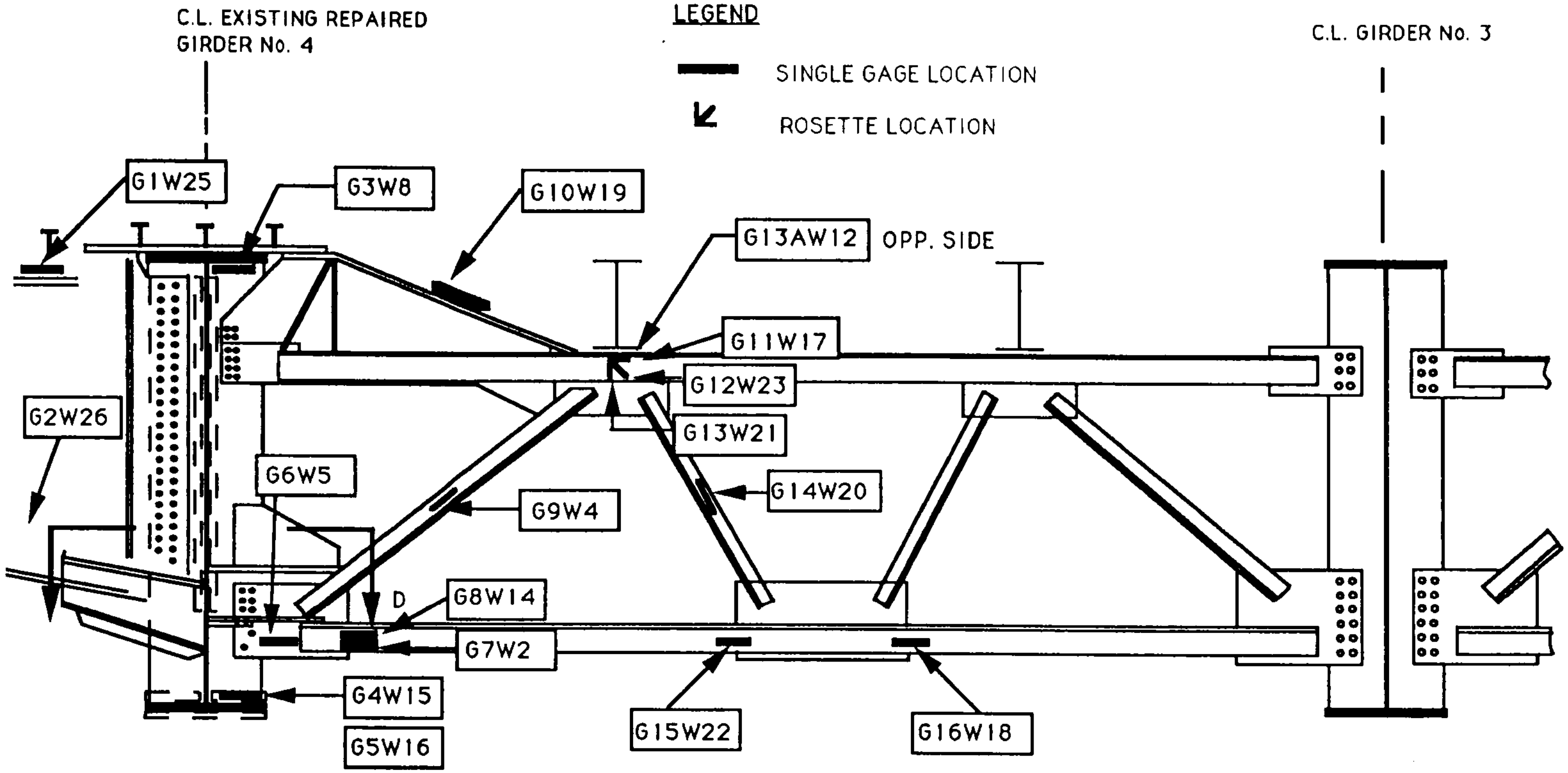

(1A) SAMPLE LOCATION # 1A

CROSS FRAME AT FAILURE LOCATION

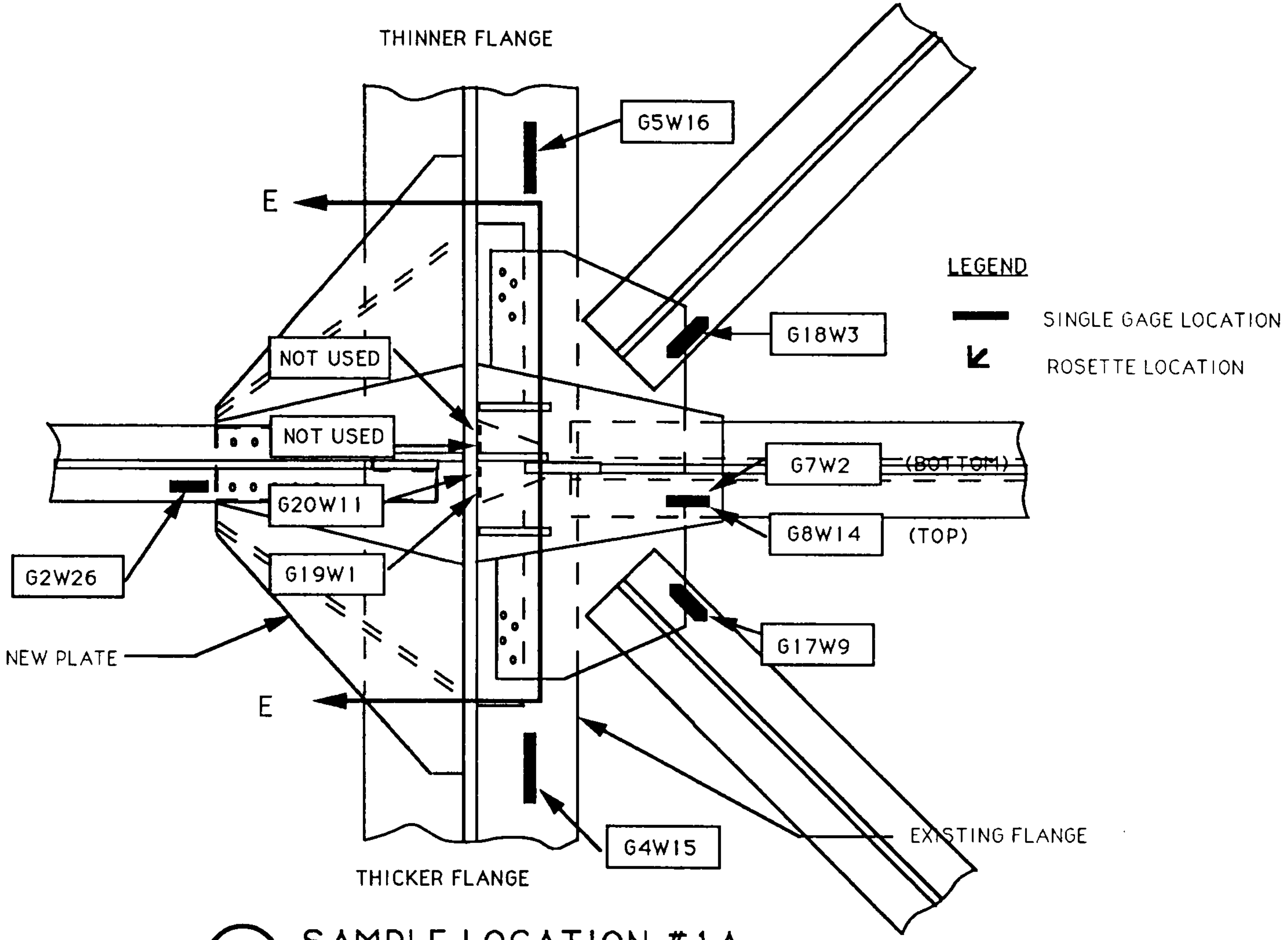

1A SAMPLE LOCATION #1A

SECTION D-D

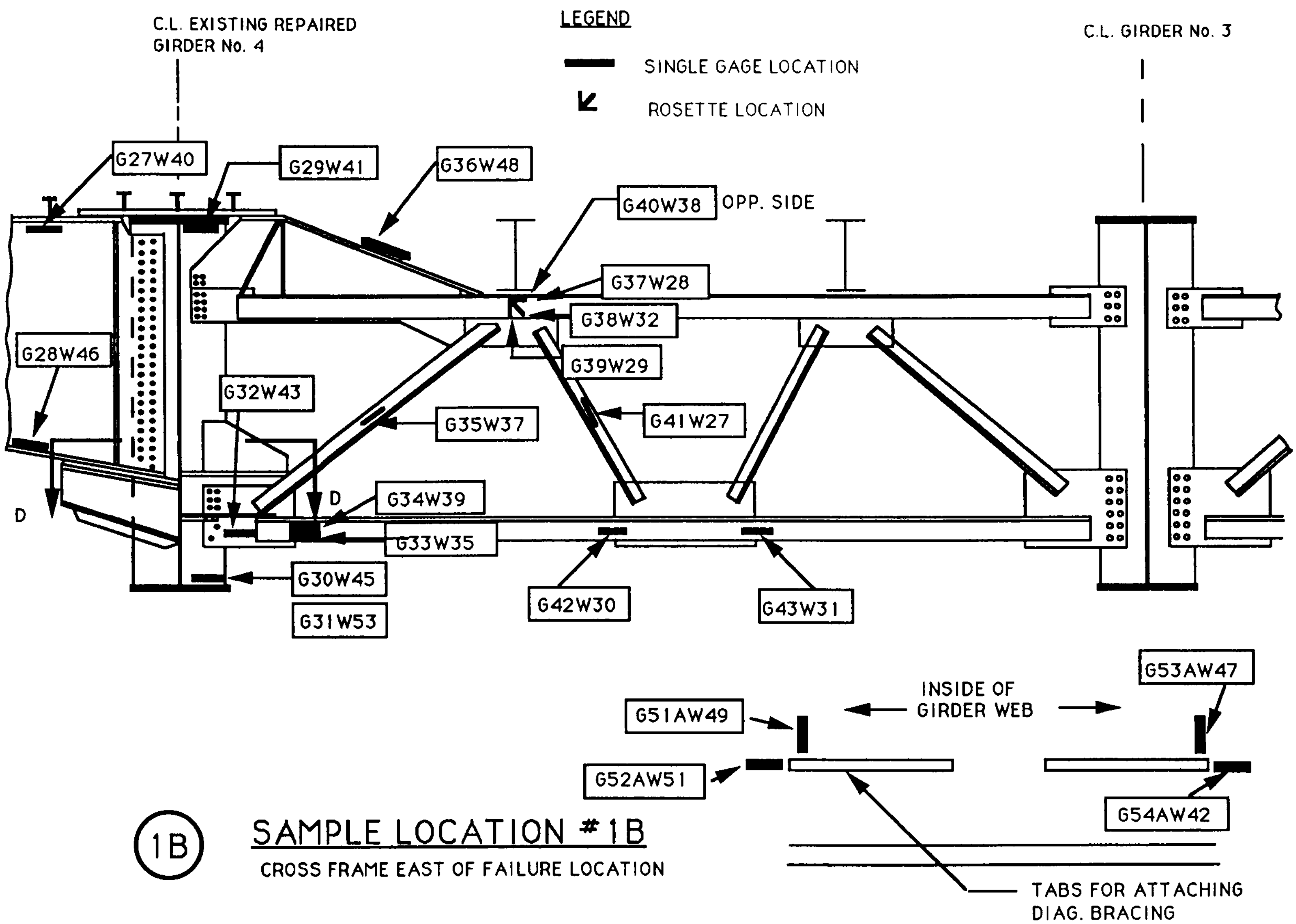

1B

SAMPLE LOCATION #1B

CROSS FRAME EAST OF FAILURE LOCATION

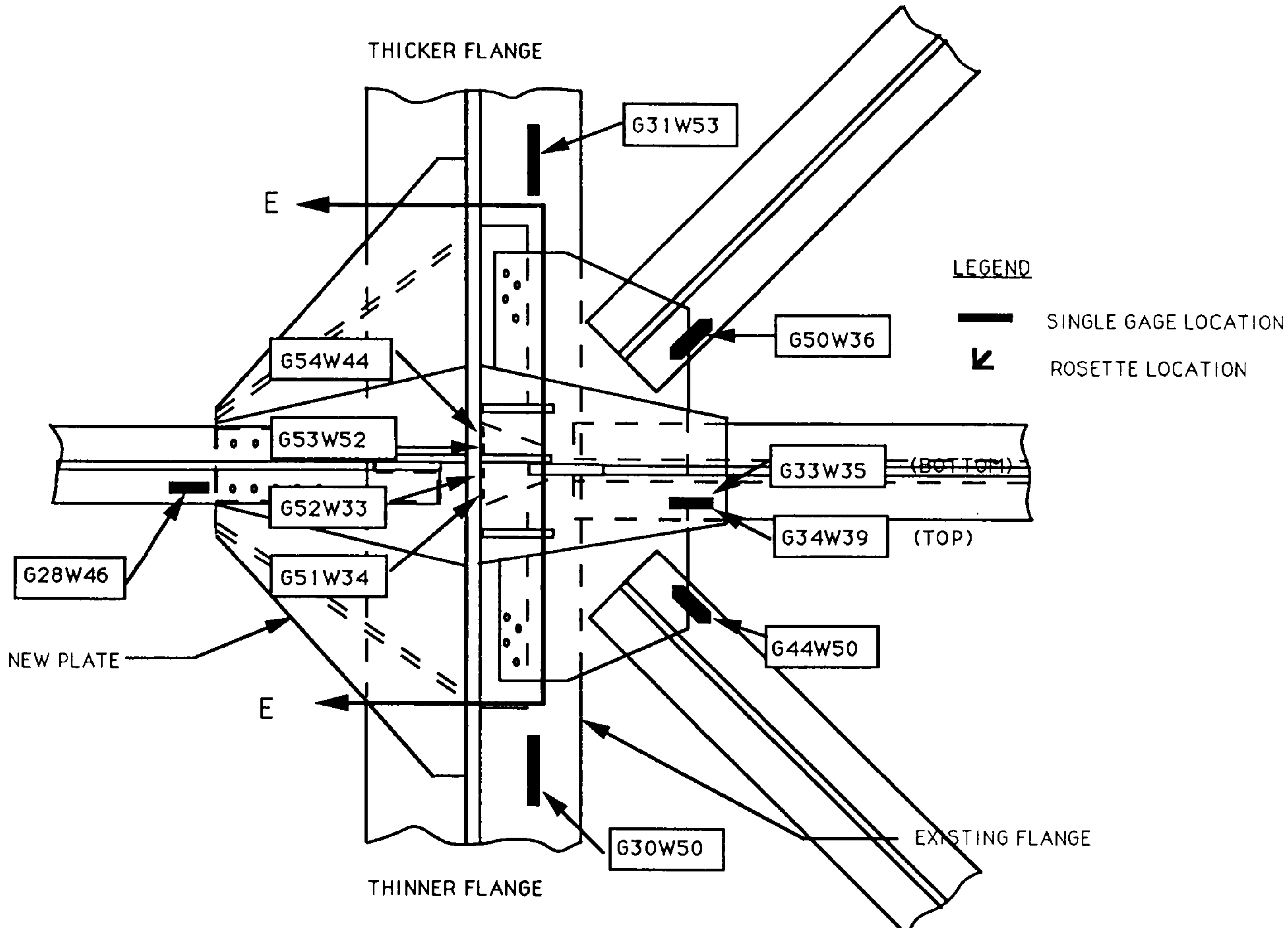

(1B) SAMPLE LOCATION #1B

SECTION D-D

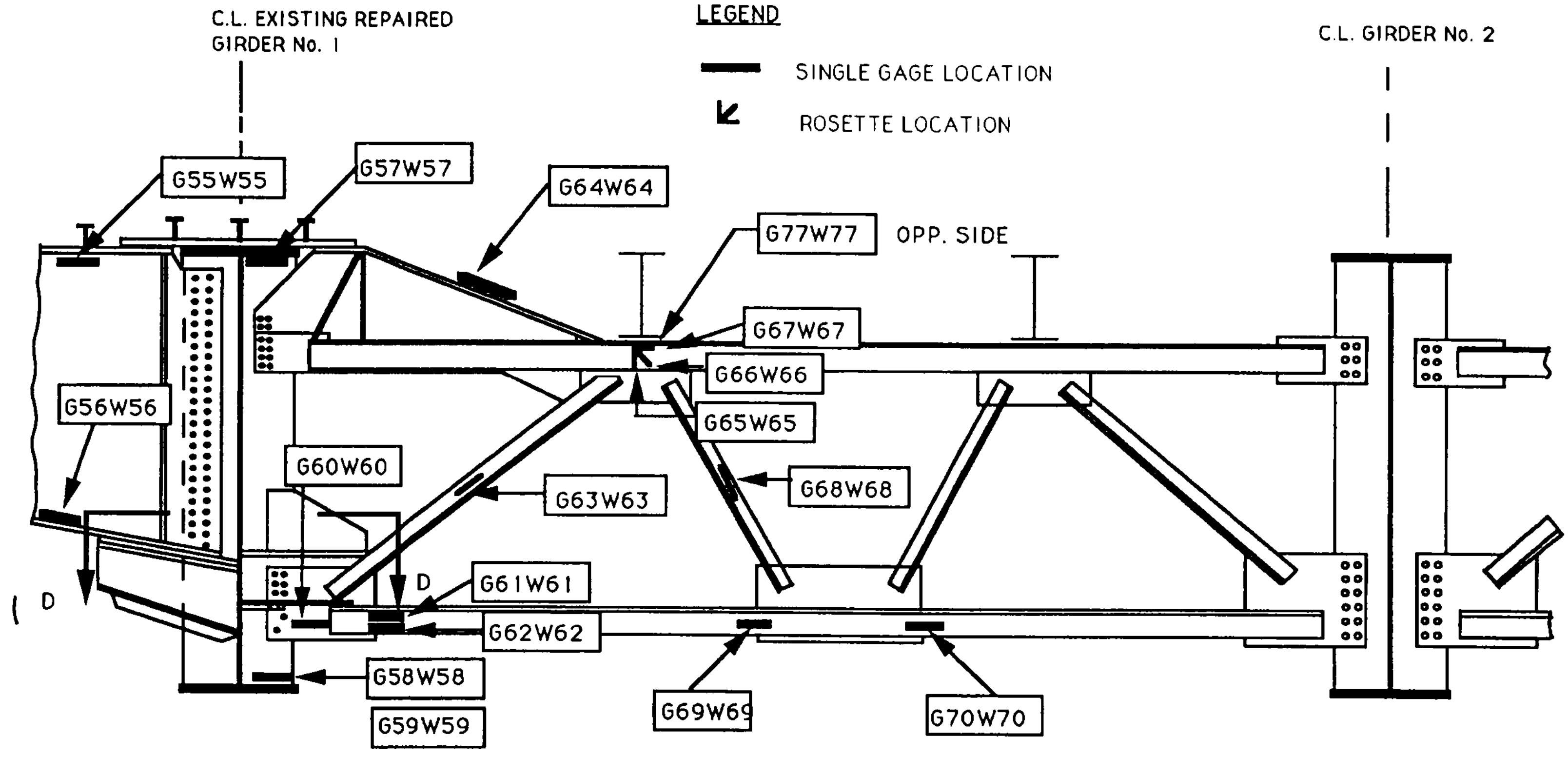

1C SAMPLE LOCATION #1C

CROSS FRAME ADJACENT TO FAILURE LOCATION

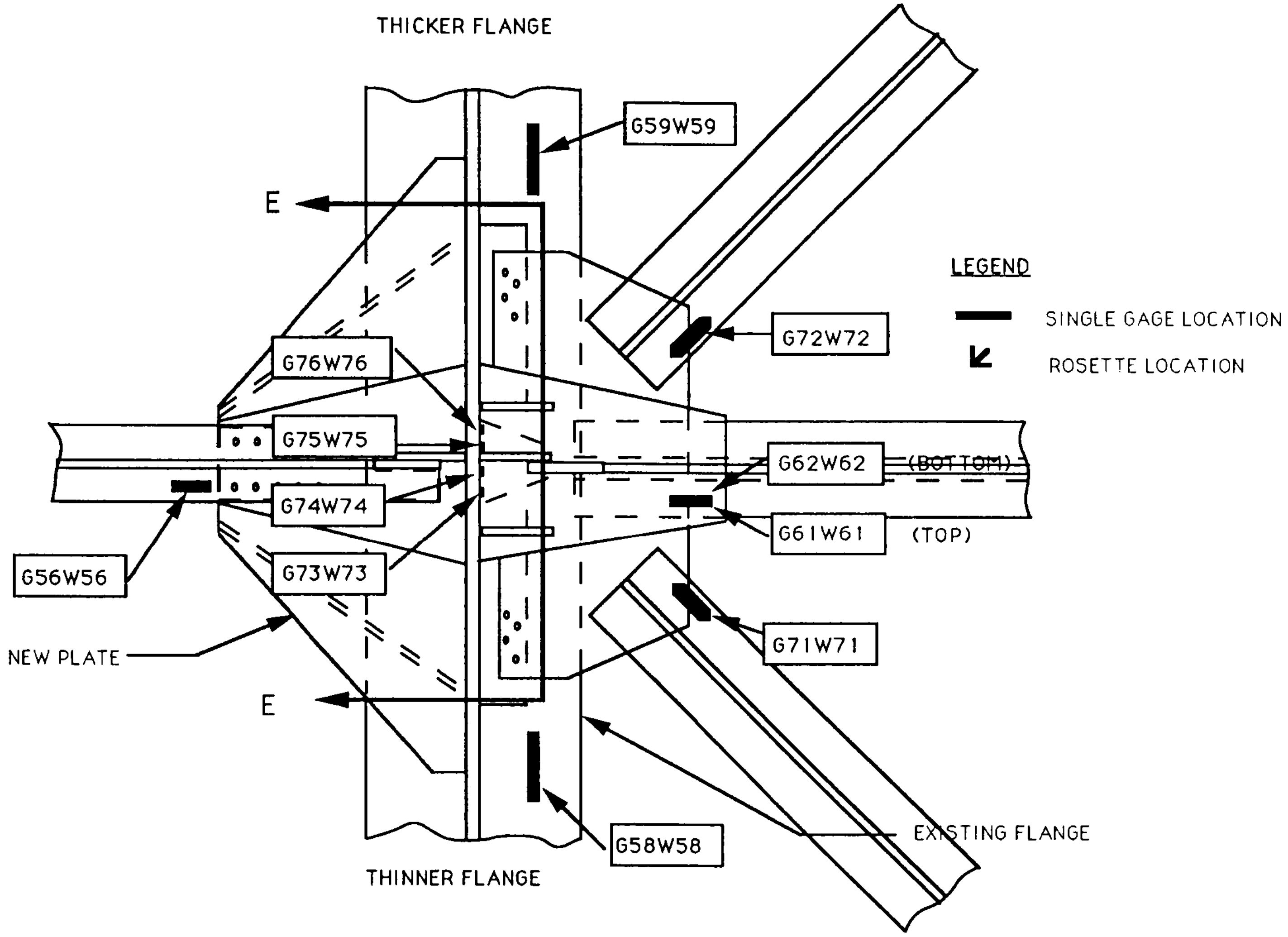

SAMPLE LOCATION #1C

SECTION D-D

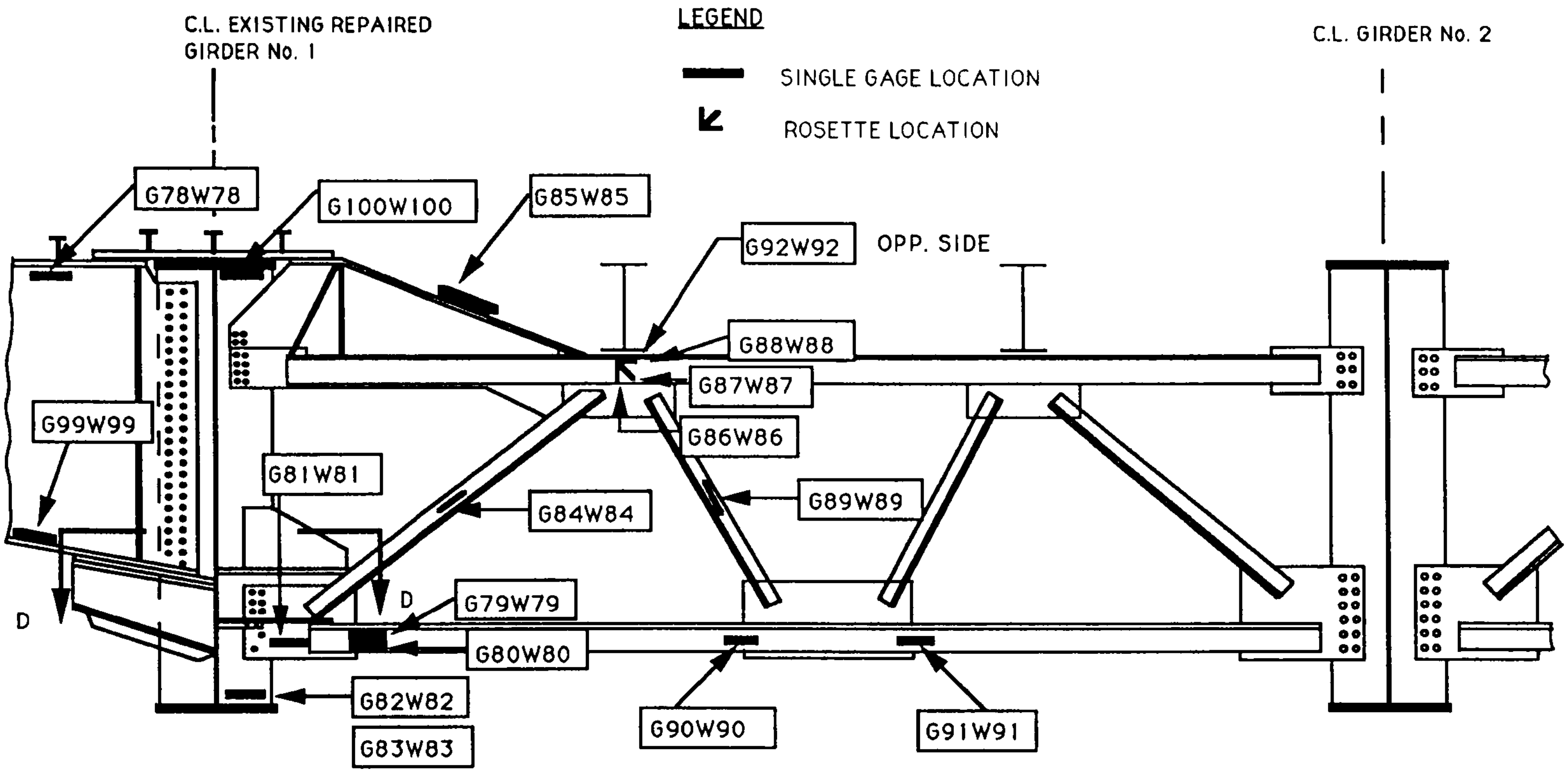

SAMPLE LOCATION # 1D

1D

CROSS FRAME WEST BOUND AND EAST OF
FAILURE LOCATION

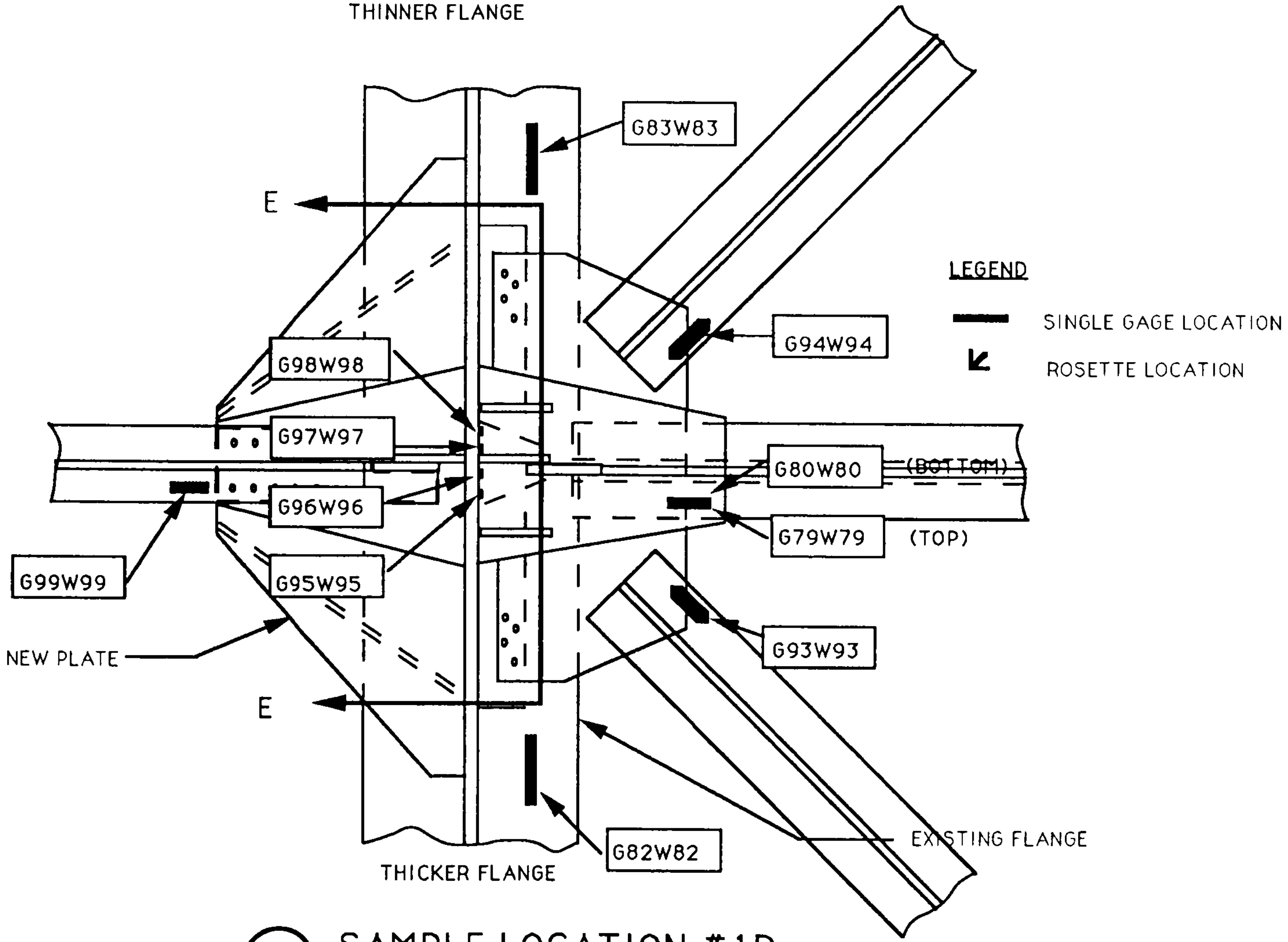

1D SAMPLE LOCATION #1D

SECTION D-D

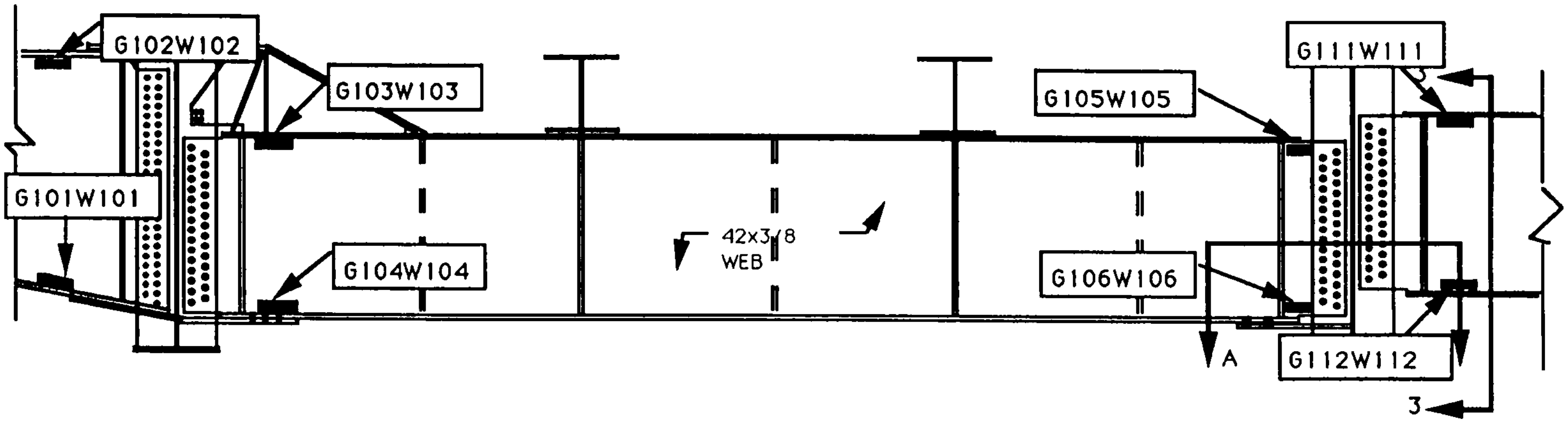

HALF SECTIONS AT FLOOR BEAMS - FB

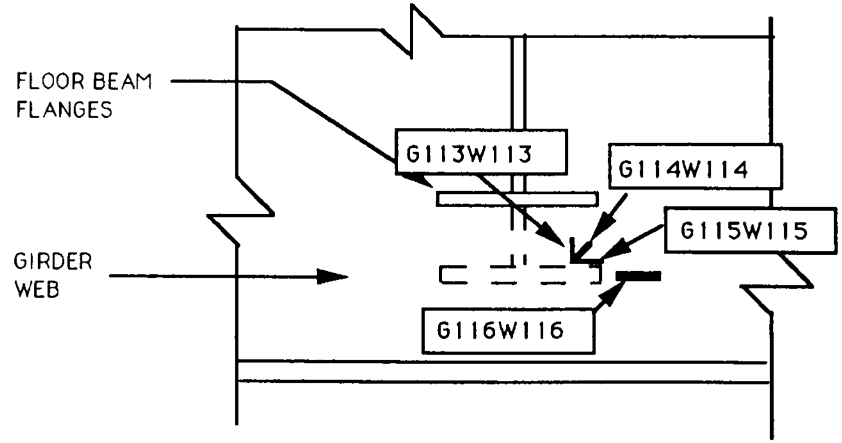

SECTION 3-3

* NOTE: LOCATION 3 WILL BE BETWEEN BEGINNNING OF BRIDGE AND PIER #1

(2) SAMPLE LOCATION #2

LEGEND

▬ SINGLE GAGE LOCATION

↙ ROSETTE LOCATION

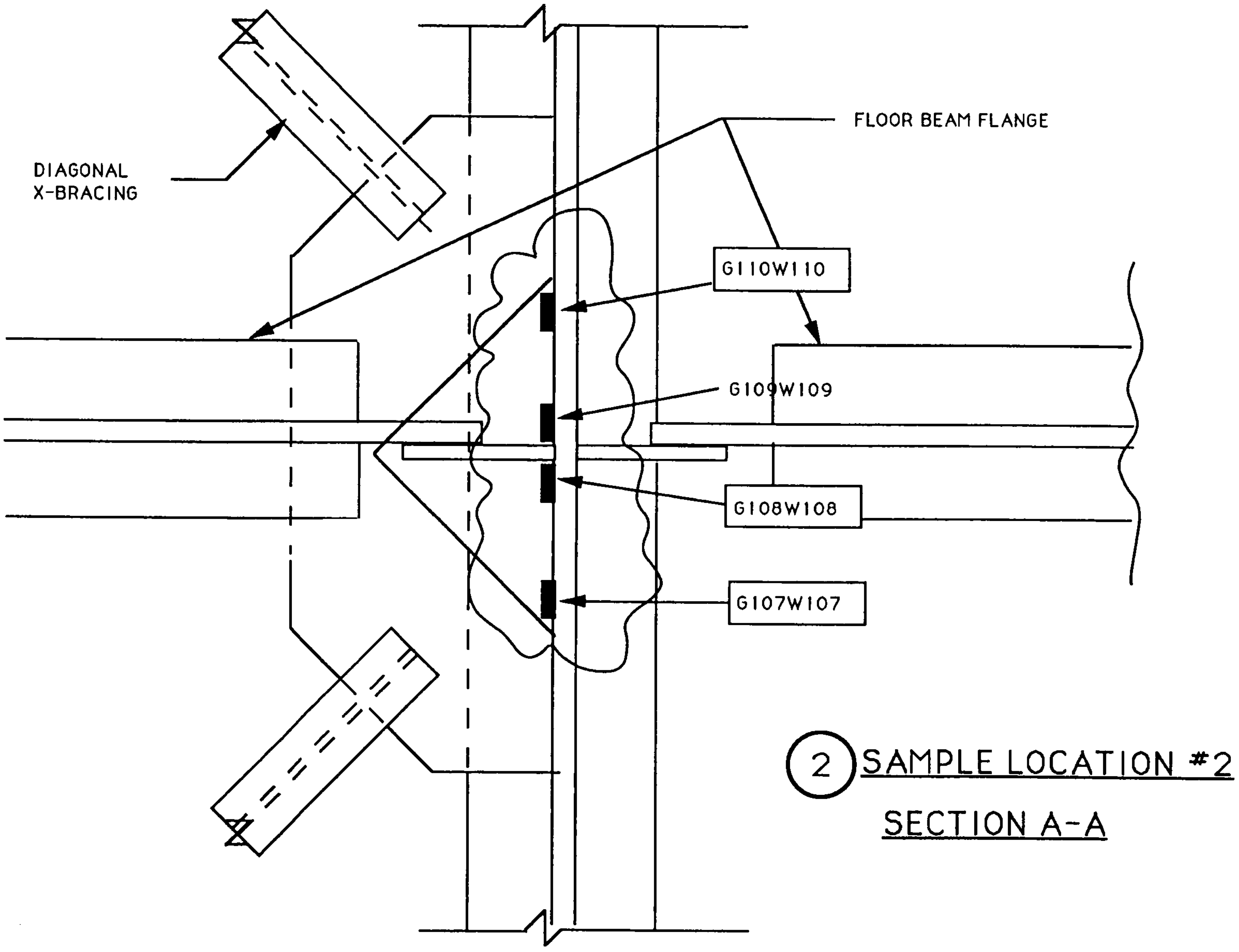

② SAMPLE LOCATION #2

SECTION A-A

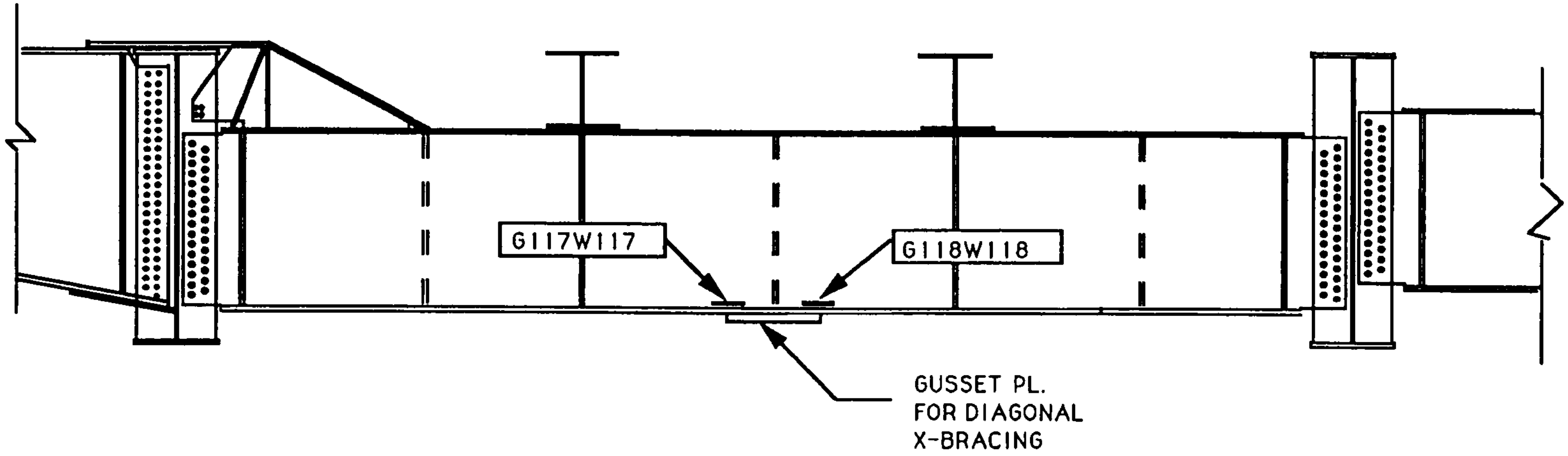

3 SAMPLE LOCATION #3

SIMILAR TO #2

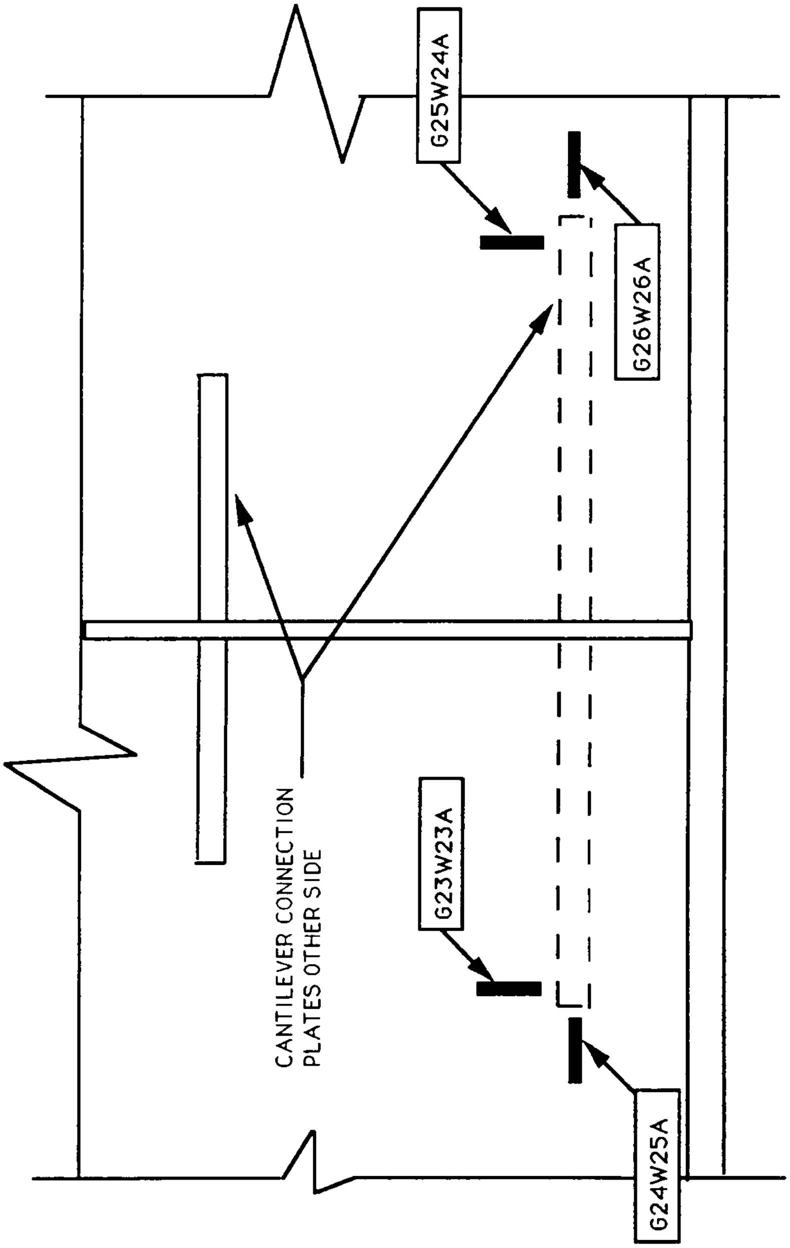

4 SAMPLE LOCATION #4

INSIDE OF GIRDER #4 WEB AT CROSS FRAME W/O
DIAGONAL X-BRACING

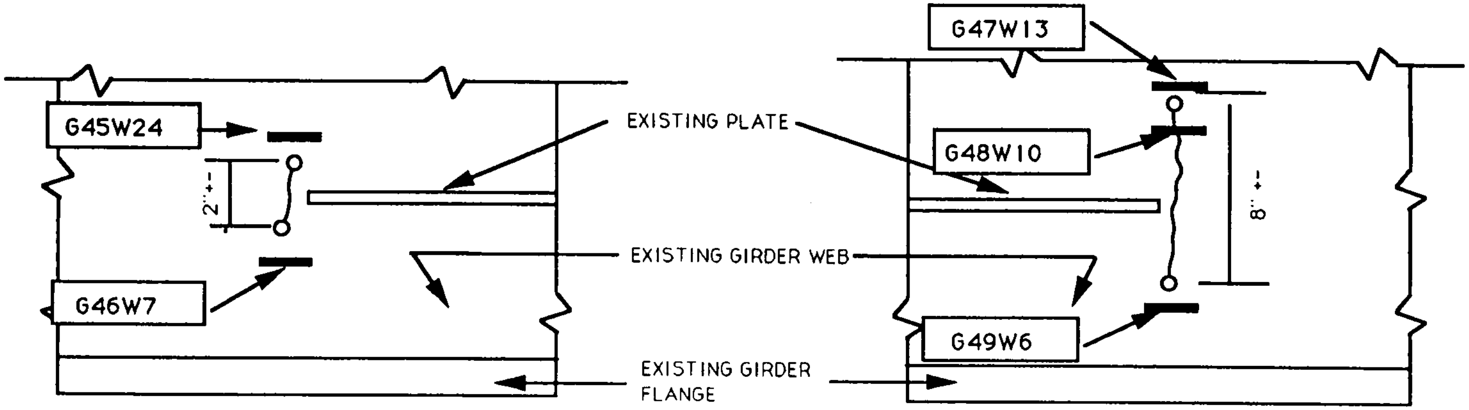

ELEVATION N-N

ELEVATION M-M

5 SAMPLE LOCATION #5
AT FAILURE LOCATION

VITA

Michael David Sanders was born in Huntingdon, Tennessee on January 25, 1968. He attended primary and elemetary schools in Huntingdon, Tennessee. He graduated from Huntingdon High School in May,1986. In August, 1986 he entered the University of Tennessee at Martin. In January, 1990 he transfered to the University of Tennessee at Knoxville and received a Bachelor of Science degree in Civil Engineering in December, 1992. In January, 1993 he entered graduate school at the University of Tennessee at Knoxville and received a Master of Science degree in Civil Engineering in May, 1994.